Characterization and Applications of Single-Domain Antibody Mimics against ErbB3

Yingqiu Zhou

A thesis submitted to the faculty at the University of North Carolina at Chapel Hill in partial fulfillment of the requirements for the degree of Master of Science in Pharmaceutical Sciences in the School of Pharmacy

Chapel Hill
2016

Approved by:

Qisheng Zhang

Albert Bowers

Rihe Liu

ABSTRACT

YINGQIU ZHOU: CHARACTERIZATION AND APPLICATIONS OF SINGLE-DOMAIN ANTIBODY MIMICS AGAINST ERBB3
(Under the direction of Rihe Liu)

As a member of EGFR family, ErbB3 is a critical heterodimerization partner of EGFR and ErbB2 in many EGFR- or ErbB2-driven cancers. As a ligand of ErbB3, heregulin β-1 (NRG1) induces the dimerization of ErbB3 with other ErbB family members and triggers downstream pathways. Using the directed protein evolution technique mRNA display, we successfully identified SDA^{HER3}-A1 and SDA^{HER3}-D5 that bind to ErbB3 with very high affinity and specificity *in vitro* and on cell surface. A biparatopic SDA^{HER3}-D5A1 was constructed for improved biophysical properties and picomolar affinity (80.3 ± 20.3 pM) to ErbB3. SDA^{HER3}-D5A1 binds to ErbB-expressing MCF7 cells with a binding affinity of 35.61 ± 17.07 nM. SDA^{HER3}-D5A1 inhibits the NRG1-induced proliferation in a dose-dependent manner. SDA^{HER3}-D5A1 is able to carry the conjugated AuNP to ErbB3-overexpressed cell and kill the cancer cell by hyperthermia treatment. Combined with Lapatinib, a kinase inhibitor, SDA^{HER3}-D5A1 showed improved efficiency in inhibiting the proliferation of cancer cells with ErbB2 and ErbB3 overexpressed. An examination of downstream signaling pathways suggested that SDA^{HER3}-D5A1 significantly decreased NRG1-induced ErbB3-/Akt-/ERK-

phosphorylation and the combination with the drug further inhibits the phosphorylation. SDA^{HER3}-D5A1-IRDye800 conjugates was synthesized and confirmed that SDA^{HER3}-D5A1 can be used to target ErbB3-overexpressed tumor xenograft models and may be very useful for imaging purpose.

To my family and friends.
Thank you so much for all of your support.

ACKNOWLEDGEMENT

I would like to thank all the people that makes this thesis possible. Five years of graduate school is such a long journey, and without the supports from my family and friends, I would never get through all the difficulties and hardship, and find a new path in my life.

I would like to express my sincerest gratitude to my advisor, Dr. Rihe Liu, and the previous and current lab members, especially to Dr. Jianwei Zou, Dr. Dongwook Kim, Dr. Adam Friedman, Lu Zhang for their continuous support and inspiration in the field of scientific research and drug discovery. Working with the team gave me invaluable experience in problem solving and critical thinking.

I really appreciate the help from my colleagues in collaborations and the staff from UNC core facilities, especially Dr. Hui Wang and Mengzhe Wang from Dr. Zibo Li's lab, Dr. Ashutosh Tripathy from UNC Macromolecular Interactions Facility, people in CICBDD, and the staff in UNC microscopy service laboratory and UNC flow cytometry core facility.

I gratefully thank my committee members, Dr. Qisheng Zhang and Dr. Albert Bowers for their kindness and advice. Ain Mason and Dr. Michael Jarstfer for their help and guidance, as well as other professors and staff in the division.

I am so grateful to my friends I met here in the pharmaceutical sciences program, especially Jingxian Chen from DPET, Xiaomeng Wan and Dongfen Yuan from MOPH for their expertise in research and spiritual supports.

Finally, I would like to take this opportunity to express the profound gratitude to my parents, my family and friends. They have been supporting me regardless of what decisions I made all through my life even being thousands of miles away.

TABLE OF CONTENTS

LIST OF TABLES x

LIST OF FIGURES xi

LIST OF ABBREIATIONS xiii

CHAPTER 1

Introduction 1

Targeted Cancer Therapy 1
The ErbB family and cancer 2
Targeting ErbB receptors for cancer treatment 5
Targeting ErbB3 and combination therapies 6

CHAPTER 2

Characterization of the pre-selected single-domain antibody mimics against ErbB3 14

Introduction 14
Materials and Methods 16
Result 19
Pre-selected SDAs with distinct sequences shows good solubility and level of expression 19
SDA^{HER3}-A1 and SDA^{HER3}-D5 showed great binding affinity to ErbB3 *in vitro* and selectively binds to ErbB3-positive cells 19
Discussion 21

ChAPTER 3

Generation and characterization of a biparatopic ErbB3 -targeting SDA^{HER3} 29

Introduction 29

Materials and Methods 31
Result 34
Construction, expression and purification of SDA^{HER3}-D5A1 and SDA^{HER3}-D5A1-Cys 34
SDA^{HER3}-D5A1 binds to ErbB3 with picomolar affinity and specificity *in vitro*, and it selectively binds to ErbB3-positive cells 34
Competition assay supported that SDA^{HER3}-D5A1 is a biparatopic molecule and binds to ErbB3 35
Cellular binding affinity of SDA^{HER3}-D5A1 to ErbB3 -positive cell line 36
SDA^{HER3}-D5A1 inhibited the NRG1 induced proliferation 36
Discussion 38

CHAPTER 4

Biparatopic ErbB3-targeting SDA^{HER3} as a theranostic agent 50

Introduction 50
Materials and Methods 52
Result 55
SDA^{HER3}-D5A1 internalized through receptor-mediated endocytosis (RME) and targeted ErbB3-positive cells in hyperthermia treatment. 55
A combination of SDA^{HER3}-D5A1 and Lapatinib showed improved inhibition efficiency in proliferation assay 55
SDA^{HER3}-D5A1 inhibited the ligand-induced activation of the downstream pathways 56
SDA^{HER3}-D5A1-IRDye800 conjugate as fluorescence imaging probe for ErbB3-expressing cancers 57
Discussion 58

CHAPTER 5

General discussion 69

REFERENCES 72

LIST OF TABLES

Table 1.1 ErbB receptor dimers and their ligands 11

Table 1.2 FDA approved small molecule drugs and antibody drugs targeting EGFR and ErbB2 12

Table 1.3 ErbB3 targeting antibodies in development and clinical trials 13

LIST OF FIGURES

Figure 1.1 ErbB family and the ligands, adapted[47] 9

Figure 1.2 Signaling pathway of ErbB receptors, adapted from cellsignal.com..... 10

Figure 2.1 Selection strategies by general elution and ligand-specific competitive elution. 23

Figure 2.2 The Changes in Recovery Percentages Show Enrichment in two Selections 24

Figure 2.3 The binding affinity of selected SDA^{HER3}s against ErbB3 ECD-Fc in vitro by ProteOn XPR36..... 25

Figure 2.4 The binding of SDA^{HER3}-A1 and SDA^{HER3}-D5 to ErbB3-positive ASPC1 cells were confirmed by confocal microscopy 26

Figure 2.5 Confocal microscopy confirmed that SDA^{HER3}-A1 and SDA^{HER3}-D5 did not bind to ErbB3-negative MDA-MB-231 cells..... 27

Figure 2.6 The WT-FN3 showed no binding to ErbB3-positive or ErbB3-negative cell lines by confocal microscopy 28

Figure 3.1 Purification of SDA^{HER3}-D5A1 and SDA^{HER3}-D5A1-Cys 40

Figure 3.2 The binding affinity of SDA^{HER3}-D5A1 to ErbB3 ECD-Fc..... 41

Figure 3.3 Selectivity of SDA^{HER3}-D5A1 to ErbB receptor family..... 42

Figure 3.4 Binding affinity of SDA^{HER3}-D5A1 against ErbB4..... 43

Figure 3.5 The binding curve of SDA^{HER3}-A1, SDA^{HER3}-D5 and SDA^{HER3}-D5A1 to the extracellular domain of ErbB4..... 44

Figure 3.6 SDA^{HER3}-D5A1 selectively binds to ErbB3-positive cell line 45

Figure 3.7 Competition experiment with confocal microscopy supported the hypothesis that SDA^{HER3}-D5A1 is biparatopic molecule 46

Figure 3.8 Flow Cytometry confirmed SDA^{HER3}-D5A1 selectively bind to ErbB3-positive cell line with good binding affinity. 47

Figure 3.9 SDA^{HER3}-D5A1 does not stimulate or inhibit the normal cell growth while it inhibits the NRG1 stimulated cell proliferation..... 48

Figure 3.10 SDA^{HER3}-D5A1 showed growth inhibition to NRG1 stimulated proliferation for ErbB3-positive cell lines selectively 49

Figure 4.1 Internalization assay confirmed that SDA^{HER3}-D5A1 bound to ErbB3 receptors and got internalized after 2 hours incubation at 37 °C 60

Figure 4.2 Hyperthermia treatment using SDA^{HER3}-D5A1-AuNP 61

Figure 4.3 Proliferation of MCF7 cells, treated with 500 nM SDA^{HER3} -D5A1, 5 μM Lapatinib, and a combination of protein and the drug 62

Figure 4.4 Proliferation of BT474 cells, treated with 500 nM SDA^{HER3} -D5A1, 5 μM Lapatinib (positive control), 25 nM Lapatinib and a combination of protein and the drug 63

Figure 4.5 Proliferation of ErbB3-negative MDA-MB-231 cells, treated with 500 nM SDA^{HER3}-D5A1, 5 μM Lapatinib (positive control), 25 nM Lapatinib and a combination of protein and the drug 64

Figure 4.6 Western blot analysis of SDA^{HER3}-D5A1 and its effect on the downstream pathways of MCF7 cells 65

Figure 4.7 Live imaging results from ASPC1 mouse xenograft models with SDA^{HER3}-D5A1-IRDye800, for 1 hour, 4 hours and 24 hours after injection. 66

Figure 4.8 The change in tumor:muscle ratio after injection of SDA^{HER3} -D5A1-IRDye800 or SDA^{HER3}-D5A1-IRDye800 with 20 fold excess of unlabeled SDA^{HER3}-D5A1 (as blocking agent) at 1 hours, 4 hours, 24 hours and 48 hours in ASPC1 mouse xenograft model (Non-blocking: N = 7, Blocking: N =2) 67

Figure 4.9 The change in tumor:muscle ratio after injection of SDA^{HER3} -D5A1-IRDye800 or SDA^{HER3}-D5A1-IRDye800 with x 20 fold excess of unlabeled SDA^{HER3}-D5A1 (as blocking agent) at 1 hours, 4 hours, 24 hours and 48 hours in PANC1 mouse xenograft model (Non-blocking: N = 3, Blocking: N = 2) 68

LIST OF ABBREIATIONS

Abl	Abelson
ADC	antibody-drug conjugate
AHC	anti-human IgG Fc Capture
Akt	Protein kinase B (PKB)
AR	androgen receptor
ATP	Adenosine triphosphate
AuNP	gold nanoparticles
BCR	break point cluster
BTC	betacellulin
cDNA	complementary DNA
CDR	complementarity determining region
CML	chronic myelogenous leukemia
CO_2	carbon dioxide
Cy5.5	Cyainine 5.5
DAG	Diacylglycerol kinase
DMSO	dimethyl sulfoxide
E. coli	Escherichia coli
EC_{50}	half maximal effective concentration
ECL	electrogenerated chemiluminescence
EDC	extracellular domain
EGF	Epidermal growth factor

EGFR	epidermal growth factor receptor
EPGN	Epigen
EPR	Epiregulin
ERK	extracellular signal–regulated kinases
FAK	Focal Adhesion Kinase
FBS	fetal bovine serum
Fc	fragment crystallizable
FDA	Food and Drug Administration
FN3	fibronectin type III domain
HBGF	Heparin-binding growth factor
HER	human epidermal growth factor receptor
HTS	high-throughput screening
IC_{50}	half maximal inhibitory concentration
IGF-1R	insulin-like growth factor 1
IgG	immunoglobulin G
IPTG	isopropyl-beta- D-thiogalactopyranoiside
K_D	dissociation constant
kDa	kilodalton
LB	lysogeny broth
mAb	monoclonal antibody
MAPK	mitogen-activated protein kinase
MEK	Mitogen-activated protein kinase 1
MET	c-Met or or hepatocyte growth factor receptor (HGFR)

mRNA	messenger RNA
mTOR	Mechanistic target of rapamycin
Neu	neuregulin
NRG1	Neuregulin-1
NSCLC	non-small cell lung cancer
OD	Optical density
PAGE	polyacrylamide gel electrophoresis
PBS	phosphate-buffered saline
PCR	polymerase chain reaction
PET	positron emission tomography
PI3K	Phosphatidylinositol-4,5-bisphosphate 3-kinase
PKC	Protein kinase C
PTB	phosphotyrosine-binding domain
PTEN	Phosphatase and tensin homolog
PTK	protein tyrosine kinase
RAF	Rapidly Accelerated Fibrosarcoma
RAS	ras superfamily
RET	rearranged during transfection
RT-PCR	reverse transcription polymerase chain reaction
RTK	receptor tyrosine kinase
SDA	single-domain antibody
SDS	sodium dodecyl sulfate
SH2	Src Homology 2

Src	Proto-oncogene tyrosine-protein kinase
STAT	Signal Transducers and Activators of Transcription
T-DM1	Trastuzumab emtansine
TCEP·HCl	tris(2-carboxyethyl)phosphine, a hydrochloride salt
TGF-α	Transforming growth factor alpha
TKI	tyrosine-kinase inhibitors
TM	transmembrane
T_m	melting point
VEGFR	vascular endothelial growth factor
WT	wild type

CHAPTER 1

Introduction

Targeted Cancer Therapy

Human cancer carries multiple mutations, including gene amplification, microsatellite instability, chromosomal aberration and aneuploidy[1]. Numerous studies have linked such mutations and aberrations with various types of cancers[2], which provides some valid background for designing targeted agents for cancer treatment. Targeted cancer therapy uses molecules to interfere specific target that plays a critical role in cancer growth and progression. Some popular targets includes kinases, cancer stem cells, microenvironment and combining targeted therapy with chemotherapy and the agents can be small molecules, antibodies or antisense inhibitors[3,4]. Among these, kinases are important targets for oncology drug discovery.

There are approximately 518 kinases encoded in human genome and many of them are involved in tumor proliferation and survival, such as ABL-fusion proteins, EGFR, KIT, PDGFR, FMS, VEGFR, FLT3, SRC-family (SFK) or cyclin-dependent kinases (CDKs)[5]. Common approaches include targeting mutations of kinases, inhibiting kinases, targeting kinases that are essential for tumor formation and maintenance in human body[6]. There are more than 150 drugs in clinical development that target kinases and many more in preclinical research[7]. Many of the

kinases inhibitors have already been approved by FDA and have reached the market for cancer treatment. From January 2012 to February 2015, there were 15 new small-molecule kinase inhibitors approved by FDA[8]. Glivec (STI1571, imatinib) was the first kinase inhibitor approved by FDA to treat leukemia by targeting BCR-Abl[9]. Recent examples include Zydelig (Idelalisib), the first PI3K inhibitor, and Lenvima (Lenvatinib) targeting VEGFR family[10–12]. There have been great successes in kinases inhibitor discovery; however, there are growing concerns regarding the development of drug resistance. Usually, the targeted kinases are very important in cell metabolism survival and carries important functions. Therefore, the genetically unstable cancer cells may undergo compensation processes. Moreover, it may also contribute to the multiple binding surfaces or action through other mechanisms[5]. For example, some imatinib-resistant CML patients carry overexpressed BCR-ABL[13]. To overcome this problem, many preclinical studies tried to unveil drug-resistance mechanisms, improve the drug pharmacokinetic/pharmacodynamics properties, develop co-targeting strategies and develop new agents[5].

The ErbB family and cancer

Tyrosine kinases are a subclass of protein kinases that transfer a phosphate group from ATP to another protein. Protein tyrosine kinases (PTK) can be categorized into two classes, receptor tyrosine kinases (RTK) and non-receptor tyrosine kinases. Receptor tyrosine kinases regulate many key functions of cells, such as cell growth, survival, organ morphogenesis, neovascularization, tissue repair and tissue regeneration[14]. They also play crucial roles in oncogenesis[15]. Human RTK has 20 subfamilies. In general, growth factors can bind and activate RTKs, and form dimeric or

oligomeric complex. One RTK from the complex phosphorylates the neighboring tyrosine from another RTK. The phosphorylated tyrosine recruits the downstream signaling proteins later[16]. The ligand-binding induced dimerization activates multiple cytoplasmic signaling pathways, such as RAS/Raf – MAPK pathway, pI3K/Akt pathway and protein kinase C pathway[4]. The other mechanism of dimerization for most RTKs includes receptor-mediated or a combination of ligand-mediated and receptor mediated mode[16]. In normal cells, the activity of RTKs is strictly regulated. However, in many cancers, some RTKs are dysregulated or constitutively activated[14]. Thus, RTKs attract many attentions from researchers as promising therapeutic targets for cancer therapies.

To become a targeted RTK for cancer treatment, the RTK itself usually is a major regulator of cancer survival and/or proliferation[14]. EGFR is one of the earliest discoveries in RTKs and related to cancer as an oncogene. In 1980s, the overexpression of EGFR was reported in many epithelial tumors, with several deletions and/or point mutations[15]. EGFR is one of the ErbB receptors. In the search of oncogenes, four ErbB family members were identified, EGFR (ErbB1, Her1), ErbB2 (Her2, Neu), ErbB3 (Her3) and ErbB4 (Her4). Figure 1.1 illustrates the four family members and its corresponding growth factor group as ligands. As shown in the figure, ErbB2 has no known natural ligand while ErbB3 lacks protein kinase domain. The structure of ErbBs includes extracellular domain, trans-membrane segment and C-terminal tail. The extracellular segment contains four domains (I-IV). Domains I and III involve in binding (except ErbB2, which lacks this two domains), while domain II is the site for dimerization. Therefore, ErbB2 prefers forming dimers with another ligand-bound

receptor[17]. As indicated above, ErbB3 is the only one in the family that does not contain kinase domain in its C-terminal tail[18].

Similar to other protein kinases, ErbB receptors are activated by forming homo-/heterodimers. Dimerized receptors phosphorylate the C terminus and trigger the downstream signaling pathways. Table 1.1 shows the ErbB receptor dimers and their ligands. The dimerization of ErbB receptors suggest an effective approach to block ErbB-mediated transformations by identifying inhibitors disrupting the interactions[19]. The ErbB family involves in many important signaling pathways, as illustrated by Figure 1.2. For example, ErbB2 and EGFR can stimulate signaling proteins and pathways, including MAPK, PI3K/Akt and mTOR pathways, Src kinase, and STAT transcription factors[20]. The dysregulation of ErbB signaling pathways, such as mutations and/or overexpression, occurs in various cancers.

The overexpression, gene amplification or mutations of EGFR are found in many cancers, such as breast cancer, lung cancer, head and neck cancers, and highly expressed in brain tumors. EGFRvIII is the most common mutation of EGFR, which has been related to resistance to radiation therapy for cancer treatment[21,22]. The association between ErbB2 and breast cancers is well studied. Clinical trials implied that women with ErbB2-positive tumors usually have poorer prognosis[23]. Overexpression of ErbB2 is also very common in other types of cancers such as ovarian, lung, pancreas, colon, esophagus, prostate, endometrium, and cervix cancers[22]. Although ErbB3 is kinase defective, it can be phosphorylated by other receptors. It plays a major role in cell survival[18] and is related to various types of cancers. The overexpression of ErbB3 has been observed in 20-30% of the invasive breast cancers[24]. The function and role of

ErbB3 in cancers are discussed in the later sections. ErbB4 is the least studied ErbB receptor in the family. Some reports suggested its prognostic value in breast cancer[25,26]. Overall, the ErbB receptor family plays an important role in cancer proliferation and progression.

Targeting ErbB receptors for cancer treatment

The ErbB receptors and its ligands locate in the extracellular domain. There are several approaches targeting ErbB receptors, directly targeting the receptor by monoclonal antibodies (mAbs) , synthetic small molecule tyrosine kinase inhibitors that inhibit the kinase domain of ErbB receptors and conjugating toxins with mABs[18,22]. ErbB receptors (except ErbB3) have inducible kinase activities at the C terminus and activate downstream pathways once activated. Even without bounded-ligand, overexpressed receptors may still have enhanced kinase activities. There are reversible and irreversible inhibitors that target the kinase domains of ErbB receptors. Reversible inhibitors compete with the binding ATPs; while irreversible inhibitors react with a cysteine residue within the ATP-binding pocket and block the kinase activity permanently[19]. mAbs usually target the extracellular domains of the ErbB receptors. Trastuzumab is the first mAb that targets ErbB2. It dramatically improve the progression and overall survival rate for ErbB2-positive breast cancer patients[27]. A third approach is to use antibody-drug conjugates (ADCs). Ado-trastuzumab emtansine is an approved antibody-drug conjugate targeting ErbB2. It contains ErbB2 targeting mAb trastuzumab, a stable thioether linker, and a derivative of toxin maytansine[18]. The antibody carries the toxin into the cell and the released toxin from the antibody kills the cell.

So far, FDA has approved six kinase inhibitors, five antibody drugs and one ADC targeting EGFR and/or ErbB2, as shown in Table 1.2. Some antibodies targeting ErbB3 are in pre-clinical and clinical trials, including mAbs against ErbB3, bispecific mAbs against ErbB3. Many of the drugs are very successful in treating ErbB2 positive tumors and non-small cell lung cancer (NSCLC) patients. However, there are observations that some patients developed resistance to trastuzumab[27] or only responded to Gefitinib or erlotinib for only 6-12 months[28]. Several mechanisms contribute to the resistance to ErbB related cancer therapies. Gefinitib and erlotinib target the EGFRs with functional mutations in the kinase domain of the C-terminus. During the treatment, the cancer cells may develop drug-sensitive mutations. Trastuzumab cannot block the signaling pathways of the cells that have autocrine EGFR activation or ligand-induced dimerization of ErbB2 and its partners. The drug resistance may also develop through activation of other RTKs or the loss of lipid phosphate PTEN, which is a negative regulator of PI3K[17,18,28,29]. New therapeutic agents or drug combination may be use to overcome the issues with drug resistance.

Targeting ErbB3 and combination therapies

The role of ErbB3 in cancer development has been intensively studied in recent years. Structurally, it is very similar to other family members, except the impaired kinase domain in the C-terminus. The ligands for ErbB3 belong to NRG family, which contains an EGF like C-terminal region and varies in N-terminus[30]. ErbB3 serves as specialized allosteric activator and signaling substrate of EGFR, ErbB2 and ErbB4[31]. In the presence of ErbB3 ligand, it promotes the kinase activity of its binding partners[32]. After dimerization, the dimerization partner phosphorylates the C-terminal tyrosine residues

of ErbB3, which can bind to SH2 or PTB binding proteins and trigger the downstream pathways later[31]. Thus, ErbB3 is a potential activator for PI3K/Akt/mTOR pathway through its tyrosine sites on C-terminus, as well as Ras/Raf/MAPK pathways[33]. The PI3K/Akt/mTOR pathway play important role in tumorigenesis and is considered a major driven factor in drug resistance of cancer treatment[34]. ErbB3 shows its significance in the ErbB2-driven tumors and the drug resistance by the upregulation of ErbB3. The upregulated ErbB3 then directly or indirectly activates the PI3K signaling pathway in those tumors[35]. ErbB3 contributes to the drug resistance to EGFR-targeted therapy by the gene amplification of MET[36]. The upregulation of ErbB3 also shows its connection to acquired resistance to RAF/MEK inhibitors in melanoma and thyroid carcinoma[35].

The overexpression of ErbB3 has been observed in primary cancers, including breast, ovarian, prostate, colon, pancreas, stomach, oral cavity and lung cancers[30]. There are direct and indirect strategies targeting ErbB3 for cancer treatment. The indirect strategies include targeting NRGs, PanHER inhibitors preventing the auto- and trans-phosphorylation of ErbB3 or targeting ErbB3 at transcriptional level[37]. As mentioned in the previous section, ErbB3 is the only member in the family that lacks functional kinase domain. Although some small molecule inhibitors were designed to target the ATP-binding region of ErbB3[38–40], the direct ErbB3 targeting strategy is by using monoclonal antibodies. Patritumab is the first human antibody targeting ErbB3, which inhibits the ligand-induced phosphorylation of ErbB3, and the downstream singling pathway of PI3K/Akt and MAPK/ERK[41]. MM-121 competes with NRG for ErbB3 binding and inhibits the ligand-induced signaling pathway[42]. LJM716 keeps ErbB3 in an inactive conformation and inhibits ligand-dependent/ligand-independent activity of

ErbB3[43]. Other antibodies may promote the degradation of ErbB3 or prevent the dimerization of ErbB2 and ErbB3[37]. Considering the physiological role of ErbB3 in ErbB network and drug resistance, some bispecific mAbs are also under development or have already been in clinical trials[44,45]. Meanwhile, combination therapies of ErbB3 antibodies and other drug agents or chemotherapies, also show some promising outcomes in clinical trials[35,46].

Figure 1.1 ErbB family and the ligands, adapted[47]

The ErbB family contains four receptors. All family members contains extracellular domain, transmembrane region and C-terminus kinase domain. However, ErbB2 does not have known ligand while the kinase activity of ErbB3 is impaired.

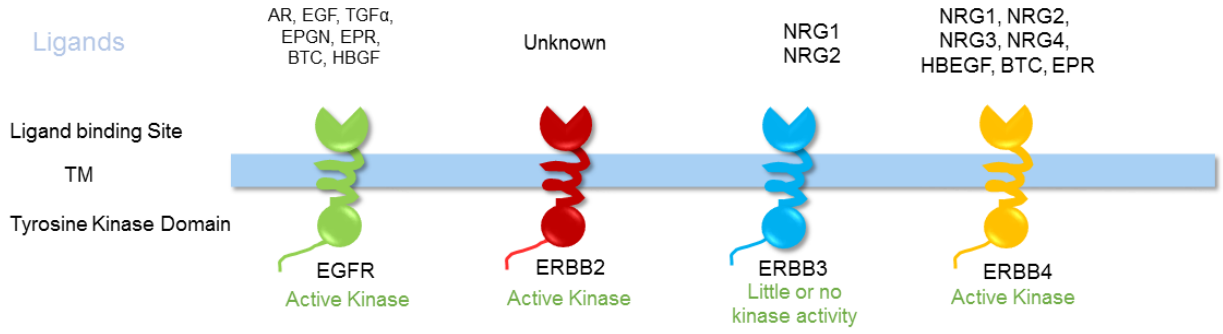

Figure 1.2 Signaling pathway of ErbB receptors, adapted from cellsignal.com

The ErbB family members activate downstream signaling pathways through homo- or hetero-dimerization. The downstream signaling pathways include MAPK/ERK, PI3K/Akt/mTOR, and other important ones, which play important role in cancer proliferation, survival and apoptosis.

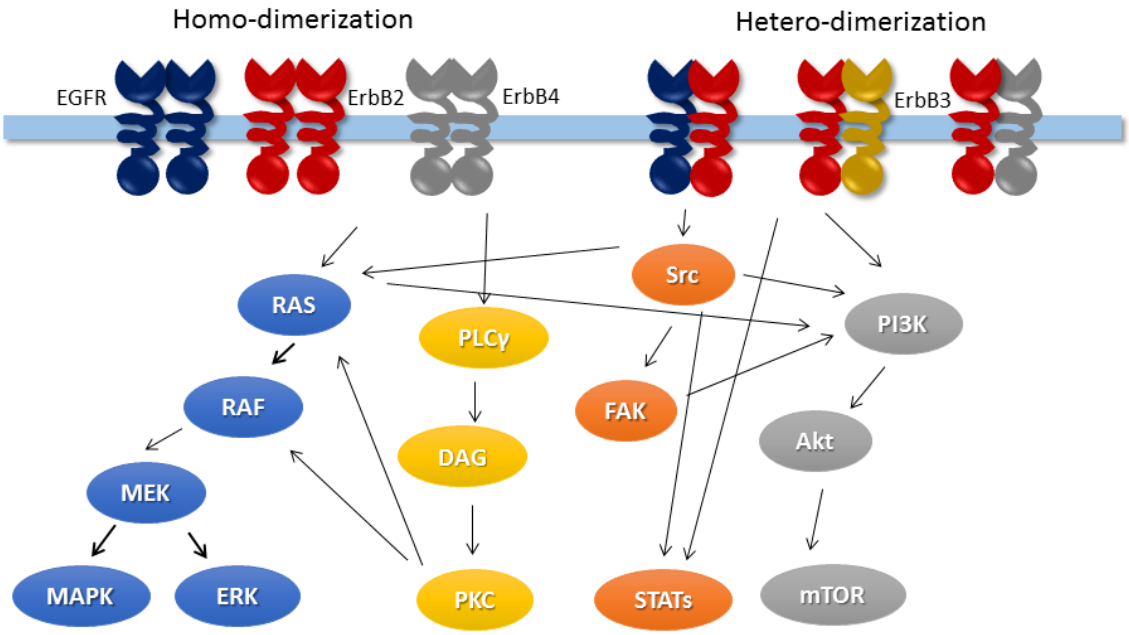

Table 1.1 ErbB receptor dimers and their ligands, adapted[18]

Receptor dimers	Ligands
ErbB1-ErbB1	EGF, EPG, TGFα, AR, BTC, HB-EGF, EPR (groups 1 and 2)
ErbB1-ErbB2	EGF, EPG, TGFα, AR, BTC, HB-EGF, EPR (groups 1 and 2)
ErbB1-ErbB3	EGF, EPG, TGFα, AR, BTC, HB-EGF, EPR, Nrg-1, Nrg-2 (groups 1, 2 and 3)
ErbB1-ErbB4	EGF, EPG, TGFα, AR, BTC, HB-EGF, EPR, Nrg-1, Nrg-2, Nrg-3, Nrg-4 (groups 1, 2, 3 and 4)
ErbB2-ErbB2	None
ErbB2-ErbB3	Nrg-1, Nrg-2 (group 3)
ErbB3-ErbB3	Nrg-1, Nrg-2 (group 3)
ErbB2-ErbB4	BTC, HB-EGF, EPR, Nrg-1, Nrg-2, Nrg-3, Nrg-4 (group 2, 3 and 4)
ErbB3-ErbB4	BTC, HB-EGF, EPR, Nrg-1, Nrg-2, Nrg-3, Nrg-4 (group 2, 3 and 4)
ErbB4-ErbB4	BTC, HB-EGF, EPR, Nrg-1, Nrg-2, Nrg-3, Nrg-4 (group 2, 3 and 4)

Table 1.2 FDA approved small molecule drugs and antibody drugs targeting EGFR and ErbB2

Drug	Company	Target	Year
Small molecules			
Afatinib/Gilotrif®	Boehringer Ingelheim	EGFR	2013
Erlotinib/Tarceva®	Genentech/OSI	EGFR	2004
Gefitinib/Iressa®	AstraZeneca	EGFR	2003
Lapatinib/Tykerb®	GlaxoSmithKline	EGFR/ErbB2	2007
Vandetanib/Caprelsa®	AstraZeneca	EGFR/VEGFR/RET-tyrosine kinases	2011
Osimertinib/Tagrisso®	AstraZeneca	EGFR	2015
Antibody			
Necitumumab/Portrazza®	Eli Lilly	EGFR	2015
Pertuzumab/Perjeta®	Genentech	ErbB2	2012
Ado-trastuzumab emtansine/Kadcyla®	Genentech	ErbB2	2013
Trastuzumab/Herceptin®	Genentech	ErbB2	1998
Cetuximab/Erbitux®	ImClone/Eli Lilly/Bristol-Myers Squibb	EGFR	2004
Panitumumab/Vectibix®	Genentech	EGFR	2006

Table 1.3 ErbB3 targeting antibodies in development and clinical trials[37]

Names	Binding Site	Blocking NRG binding
In clinical trials		
MM-121 (Seranbitumab)	Unknown	Yes
U3-1287 (Patritumab)	Unknown	Unknown
LIM716	Between domains II-IV	No
AV-203	Unknown	Yes
REGN1400	Unknown	Yes
GSK2849330	Domain III	Yes
RG7116 (Lumretuzumab)	Domain I	Yes
Under development		
TK-A3 and TK-A4	Domains II / Unknown	Yes/Yes
MP-RM-1 (EV-20)	Unknown	No
9F7-F11 and 16D3-C1	Domain I / Domain I	No/Yes
NG33	Unknown	Yes
A5/F4	Domains I & III	Yes
Bispecific Abs in clinical trials		

Name	Target
MM-111	ErbB2 & ErbB3
MEHD7945A (Duligotuzmab, RG7597)	EGFR & ErbB3
MM-141	IGF-IR & ErbB3

CHAPTER 2

Characterization of the pre-selected single-domain antibody mimics against ErbB3

Introduction

Directed evolution is an effective approach to select or improve biomolecules with desired properties. The evolution of protein/peptides *in vitro* mimics the biological evolution. The steps includes diversify genetic codes, screen and identify the potential candidates[48]. The current methods for protein selection includes Yeast two-hybrid system, phase display, cell surface display and ribosome display[49]. mRNA display covalently connect mRNA with its translated protein through puromycin analogue[50]. Different diversified libraries are used for laboratory evolution. Human fibronectin (FN3) is an extremely abundant extracellular protein that occurs in approximately 2% of all human proteins in cell surface receptors. The tenth type III domain of FN3 appears to be an ideal scaffold for the development of natural ligand competitors by using directed evolution, due to its small size (less than 10 kDa), CDR-like ligand binding surface loops, lack of disulfide bonds, high expression level in bacteria, exceptional thermostability (T_m ~90 °C), and little immunogenicity[51,52]. In the present study, we used mRNA display technique to select a fibronectin type III (FN3) domain-based library and identified proteins that can bind to ErbB3.

Two mRNA-display based selections were performed, as shown in Figure 2.1. For general elution approach, we directly collected the selected fusion molecules from the ErbB3-beads after washing. For the Ligand-specific approach, we performed competitive elution by using NRG β-1, which should elute fusion molecules that bind specifically to the NRG binding site on ErbB3. The recovery of the selected molecules was determined by the ratio of radioactivity from elution to that from total library used for selection. In general, the recovery was very low due to the high-diversity of the original library. After several rounds of selections, a significant increase in recovery indicated the successful enrichment of SDA^{HER3} sequences with desired features, as shown in Figure 2.2. This study focuses on protein identification and characterization from this selected library.

Materials and Methods

Sequencing the selected FN3 library against ErbB3

The gene coding selected FN3 molecules were sub-cloned into pJET1.2/blunt plasmid (Thermo Scientific). The resulting plasmids were transformed into DH5α Competent *E. coli* (New England BioLabs). Single clones were picked and grown in 96 well plates with LB media at 37°C overnight. The cells were amplified with PCR. The PCR products were collected and got sequenced (Eton Bioscience Inc.). Unipro UGENE v1.10.1 and ClustalW2 were used for sequence alignment and analysis.

Construction, expression and purification of soluble SDA molecules

The coding genes of the selected SDA^{HER3}s were amplified and assembled to a fusion gene through PCR using primers (5'-GAGGATCCGTGTCTGATGTTCCGCGTGAT-3', 5'-GAGCGGCCGCTTACTTGTCGTCGTCGTCCTTGTAGT-3'). The generated products were firstly ligated to pJET1.2/blunt plasmid and then later ligated to the BamH I & Not I (New England BioLabs) sites of pET28b plasmid. The resulting plasmids were further confirmed by DNA sequencing (UNC genome analysis facility) and transformed to *E.coli* BL21 (DE3) competent cells (New England BioLabs). Cells were grown in LB media with kanamycin at 37 °C until OD ~0.6 (600nm) and then induced with 0.3 mM isopropyl-beta-D-thiogalactopyranoiside (IPTG) at 20 °C for 16 h. The purification process was performed as described in the previous work in our lab[53]. Each SDA^{HER3}-A1 and SDA^{HER3}-D5 have two versions including one version with one cysteine in the C-terminus. For protein labeling, the SDA^{HER3}s (SDA^{HER3}-A1-Cys, SDA^{HER3}-D5-Cys) were first incubate with TCEP·HCl (Thermo Scientific) with 1:2 ratio, for 30min at room

temperature. A molar ratio of 1:10 was used to incubate the SDAs and Alexa-Fluor 555 C2 maleimide (Life technologies) at 4 °C overnight. Illustra NAP-5 Columns (GE healthcare) were use remove the excessive dyes. The process of the purified SDAs (Wildtype-FN3) labeling with Alexa-Fluor Fluor 555 carboxylic acid, succinimidyle ester (Life technologies) was described in the previous work[54].

Kinetic binding analysis of SDAs

ProteOn XPR36^{TM} array system (Bio-Rad) was used for kinetic binding analysis of SDA^{HER3}s. The soluble extracellular domain of human recombinant ErbB3 EDC-Fc and EGFR EDC-Fc were purchased from R&D Systems. SDA^{HER3} samples were prepared as described above. Each receptor was diluted with 10mM sodium-acetate buffer at pH 5. The immobilization of ErbB3 and EGFR were performed on a GLM sensor chip (Bio-Rad) through amine coupling approach[55]. Five different SDA^{HER3} concentration (from 200nM to 12.5nM in two-fold dilution) were injected over the immobilized Fc-ErbB3 channel and EGFR channel. The dissociation constant (K_D) were calculated by the software with 1:1 binding model.

Cell culture

ErbB3-positive ASPC1, MDA-MB-453 and ErbB3-negative MDA-MB-231, SKOV3 were obtained from UNC Tissue Culture Facility. Each cell line was cultured by serial passage with proper media in 5% CO_2 incubator, at 37 °C.

Confocal microscopy

Each cell line (about 2 x 10^4) was plated on glass coverslides and grew in media overnight. The coverslides were washed with 1 x PBS twice before incubating with different concentration of Alexa-Fluor 555-labeled SDA^{HER3}s for 30 min on ice, or for 2 h

at 37 °C. The coverslides were then washed with 1 x PBS for three times. The samples were examined with Zeiss LSM 700 confocal microscopy at UNC Microscopy Services Laboratory (MSL).

Result

Pre-selected SDAs with distinct sequences shows good solubility and level of expression

In this study, the FN3 scaffold-based SDAs that bind to the NRG1-binding site on ErbB3 were evolved from an mRNA-displayed human FN3 domain library with a diversity of 5×10^{13}. Two different selections were performed, including the general elution and the ligand-specific elution approach. The selected library members were amplified and sequenced. With simple clustering approach, five classes of SDA^{HER3}s with the following sequences were selected. The selected sequences were amplified and inserted into protein expression vectors containing His-tag for purification. All five proteins were expressed and purified. The expression level of most of the selected SDA^{HER3}s were good and were soluble as well. Initial binding tests against ErbB3 were performed to exclude the weak binders and those with poor solubility (data not shown). Among the five sequences, SDA^{HER3}-A1 was the dominant sequences (~50%) from the general elution approach after eight rounds of selection; while the sequence of SDA^{HER3}-D5 presented in both of selections and was the major sequence in ligand-specific elution approach after nine rounds of selection. Both the two SDA^{HER3}s, SDA^{HER3}-A1 and SDA^{HER3}-D5, were selected for further characterization.

SDA^{HER3}-A1 and SDA^{HER3}-D5 showed great binding affinity to ErbB3 *in vitro* and selectively binds to ErbB3-positive cells

SDA^{HER3}-A1 and SDA^{HER3}-D5 were expressed and purified for characterization. For labeling purpose, SDA^{HER3}-A1-Cys and SDA^{HER3}-D5-Cys were constructed, expressed and purified. ProteOn XPR36 was used to determine the binding affinity of

SDA^{HER3}s to ErbB3. Both SDA^{HER3}-A1 and SDA^{HER3}-D5 did not bind to immobilized EGFR-ECD-Fc (data not shown). The K_D of SDA^{HER3}-A1 and SDA^{HER3}-D5 were 1.50 ± 0.38 nM and 4.14 ± 0.20 nM, respectively (Figure 2.3). The binding mode of the two SDA^{HER3}s may be slightly different. Although the on-rate constants were similar, the off-rate constant of SDA^{HER3}-D5 was greater than that of SDA^{HER3}-A1. Overall, both SDA^{HER3}s have nanomolar binding affinity to ErbB3 *in vitro*.

Binding to the purified receptors in vitro does not guarantee the binding to the native receptors on the surface of cells. To confirm the binding of SDA^{HER3}s to ErbB3 receptors on the surface of cancer cells, confocal cell binding assays were performed with Alexa-Fluor 555-labeled SDAs. Four cell lines were used in this experiment. ASPC-1 and MDA-MB-453 cells were with high expression of ErbB3 while MDA-MB-231 and SKOV3 cells were with very low expression of ErbB3. To exclude the non-specific binding outside the randomized loops, wild-type FN3 proteins were expressed, purified and labeled. As illustrated in Figure 2.5, 500 nM and 1 μM labeled SDA^{HER3}-A1 and SDA^{HER3}-D5 all showed binding to the ErbB3-positive ASPC1 cells. However, none of them bound to the ErbB3-negative MDA-MB-231 cells (Figure 2.6). Figure 2.7 shows that 1 μM labeled wild-type FN3 proteins bound to neither ErbB3-positive (MDA-MB-453) or ErbB3-negative (SKOV3) cells. It suggested the backbone structure of FN3 proteins do not have non-specific binding to the selected cell lines. The selected SDA^{HER3}s selectively bind to ErbB3-positive cell line and may be very useful for further development and application.

Discussion

Most of the known agents that bind to ErbB3 in pre-clinical and clinical development are based on mAbs[37]. However, the process of producing mAbs and the properties of antibodies may limit the potentials in modification and further development. Therefore, smaller proteins with high expression and minimum immunogenicity may be great tools for research investigation. Göstring and his colleagues presented an affibody-based agent that bind to ErbB3 through phage display[56,57]. Affibody is a structure based on Z domain of protein A, with three α-helices and a size of approximate 6 kDa. Generally, its binding ability comes from the randomization of 13 amino acids located on the two helices[58]. The size of the affibody and the limited number of randomization region may be a limitation for its application. In contrast, FN3-based protein has larger size and three loops that can be randomized. Moreover, there is an FN3-based scaffold based drug and it has already been in clinical trials for treatment[59]. In the present study, the two mRNA-display selections based on FN3 library successfully identified some proteins with distinct sequences. The SDA^{HER3}s identified by the general elution approach may bind to any position of the extracellular domain of ErbB3; while SDA^{HER3}s selected from the ligand elution approach may be able to compete with NRG1. The design and the purpose of the second approach is to find SDAs that have similar binding affinity to NRG1 and share the same/partial binding site of NRG1. SDA^{HER3}-D5 was screened via the later approach. The binding affinity of SDA^{HER3}-D5 is relatively close to the binding affinity of NRG1 to ErbB3 (5.4 nM[60]), which is quite consistent with the experiment design. On the contrary, the general elution may screen SDAs that have much higher binding affinity to ErbB3 than NRG1. As a result,

SDA^{HER3}-A1 from general elution approach has ~ 4 folds higher binding affinity to ErbB3. Interestingly, SDA^{HER3}-A1 has a higher *k*-on rate and lower k-off rate than those of SDA^{HER3}-D5 *in vitro*. Regarding the cellular binding, the wt-FN3 protein was used as a control to rule out the backbone structure that contributes to the ErbB3 binding. In confocal microscopy study, both SDA^{HER3}-A1 and SDA^{HER3}-D5 selectively bound to the receptor on the surface of ErbB3-positive cell line in a concentration dependent manner. Overall, the experiment results suggested the selections were successful and we identified two SDA^{HER3}s, SDA^{HER3}-A1 and SDA^{HER3}-D5, that selectively bind to ErbB3 receptor with high affinity.

Figure 2.1 Selection strategies by general elution and ligand-specific competitive elution.

The general elution approach is designed to amplify and select SDAs that bind to the extracellular domain of ErbB3; the ligand-specific competitive elution selected SDAs that bind to ErbB3 and may be competed off the ligand by NRG1, which suggested the SDAs might share binding site with NRG1.

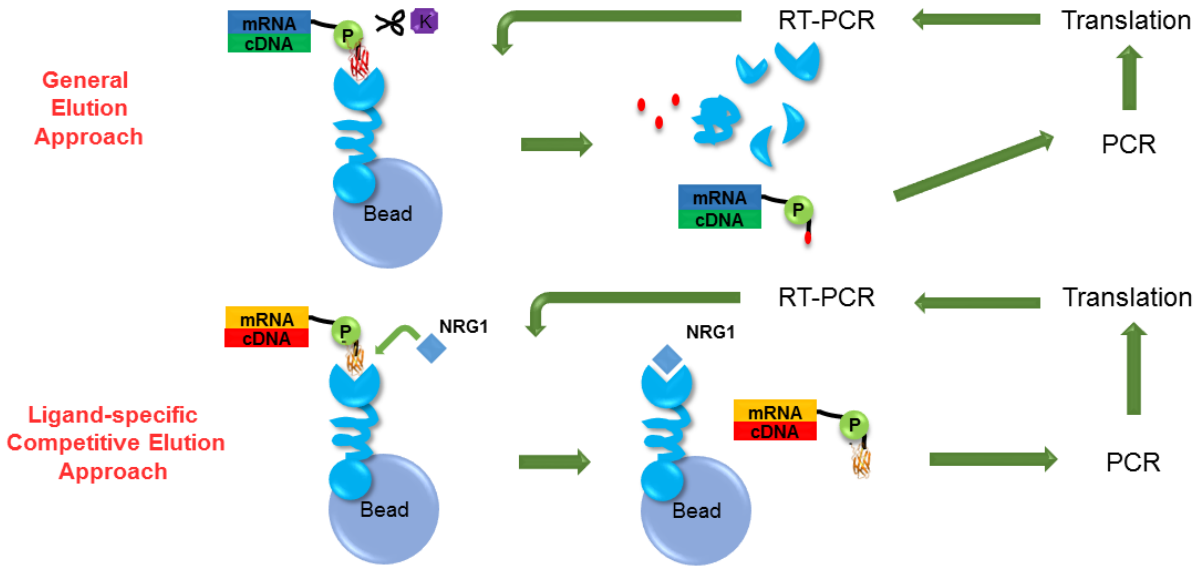

Figure 2.2 The Changes in Recovery Percentages Show Enrichment in two Selections

The change in recovery percentage from general (left) and ligand-specific (right) elution approaches through rounds of selections. The recovery rates reached 33.2% at round 8 in general elution approach and 19.8% at round 9 in ligand-specific elution approach, respectively.

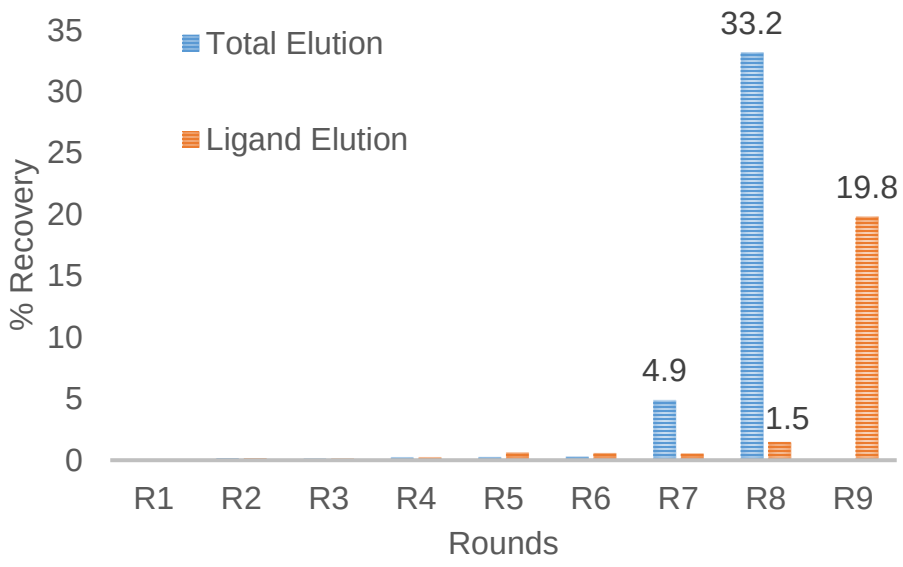

Figure 2.3 The binding affinity of selected SDA^{HER3}s against ErbB3 ECD-Fc in vitro by ProteOn XPR36

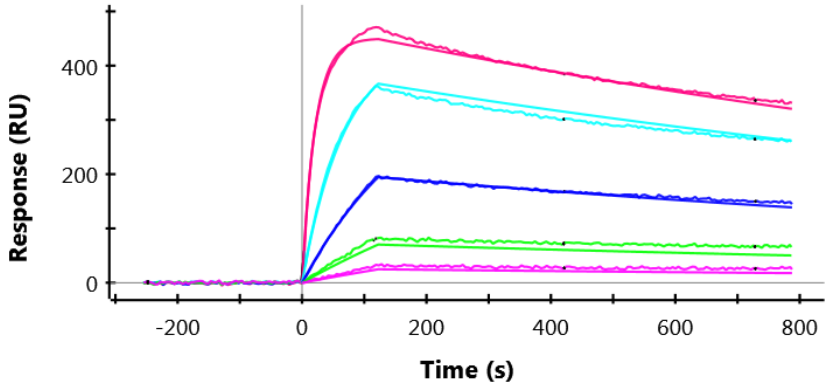

(a) Binding affinity for SDA^{HER3}-A1 against ErbB3 was 1.50 ± 0.38 nM

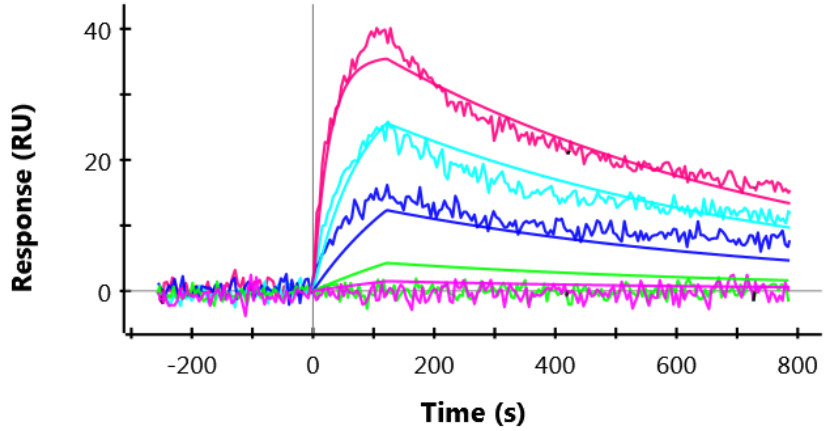

(b) Binding affinity for SDA^{HER3}-D5 against ErbB3 was 4.14 ± 0.20 nM

Figure 2.4 The binding of SDA^{HER3}-A1 and SDA^{HER3}-D5 to ErbB3-positive ASPC1 cells were confirmed by confocal microscopy

The SDA^{HER3}-A1 and SDA^{HER3}-D5 were labeled with Alexa-Fluor 555 through the reaction between cysteine residue and maleimide, and showed concentration dependent binding to the ASPC1, a pancreatic cancer cell line with ErbB3 overexpressed.

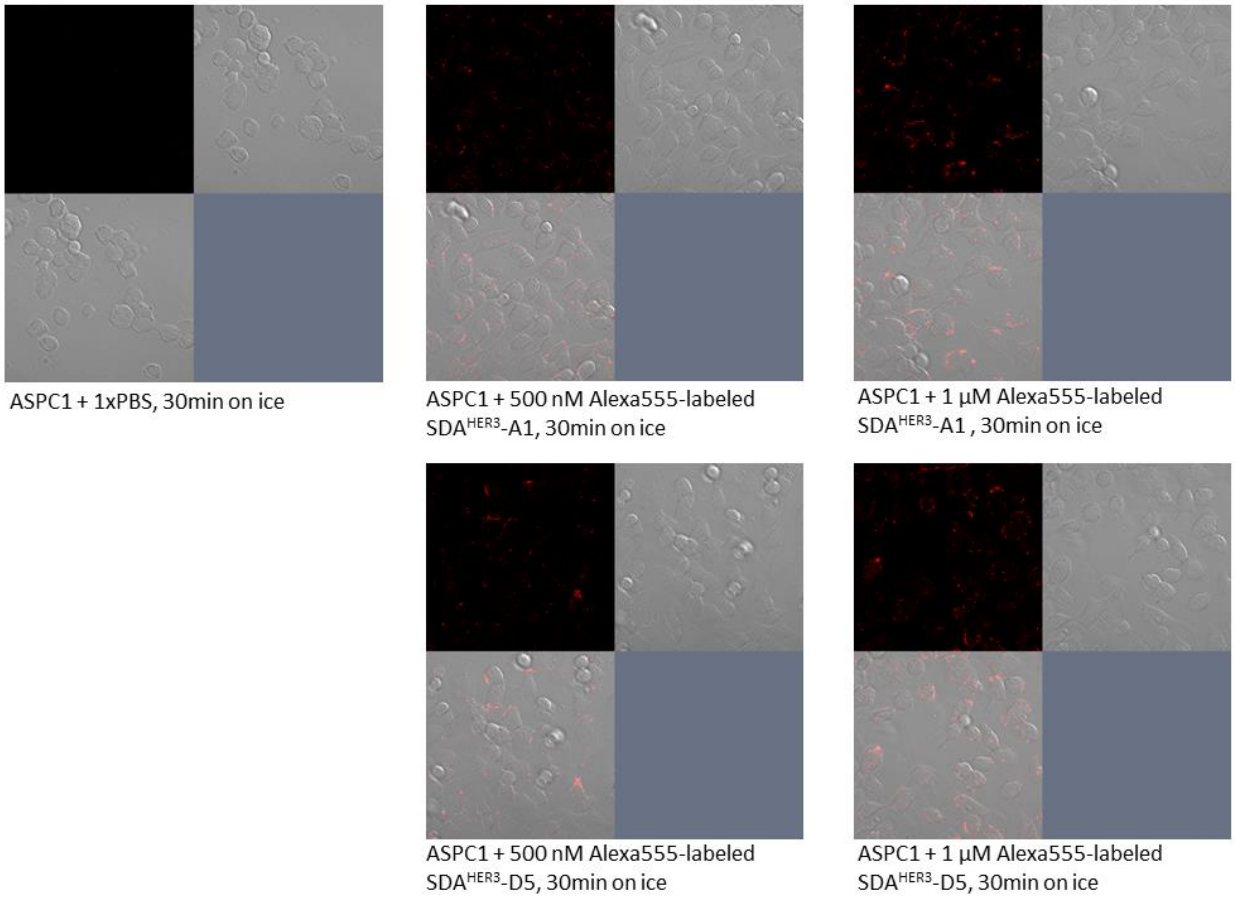

Figure 2.5 Confocal microscopy confirmed that SDA^{HER3}-A1 and SDA^{HER3}-D5 did not bind to ErbB3-negative MDA-MB-231 cells

The SDA^{HER3}-A1 and SDA^{HER3}-D5 were labeled with Alexa-Fluor 555 through the reaction between cysteine residue and maleimide, and showed no binding to MDA-MB-231, a breast cancer cell line, with no/minimum ErbB3 expression.

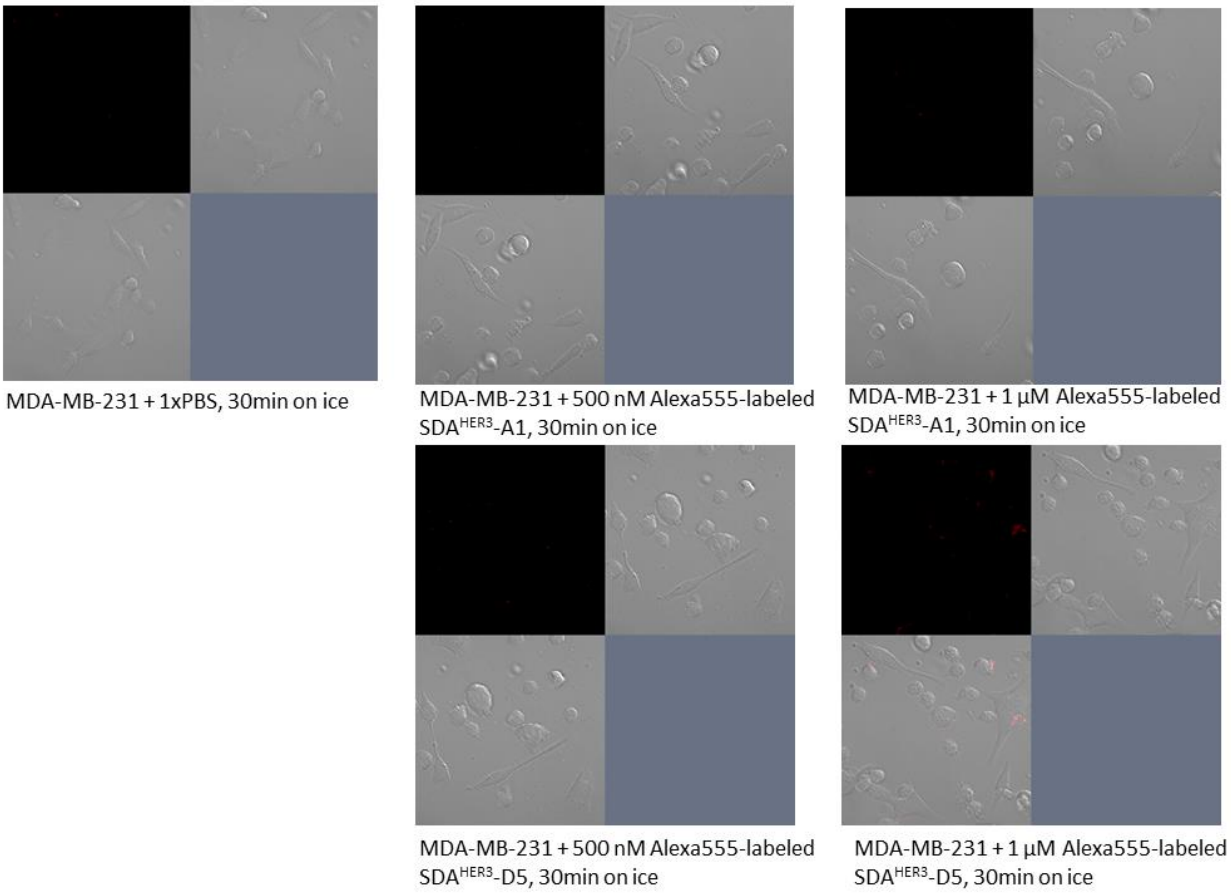

Figure 2.6 The WT-FN3 showed no binding to ErbB3-positive or ErbB3-negative cell lines by confocal microscopy

The WT-FN3 protein was labeled with Alexa-Fluor 555. It showed no binding to MDA-MB-453 (ErbB3+, breast cancer) or SKOV3 (ErbB3-, ovarian cancer), which exclude the possibility that the binding comes from the backbone structure of FN3.

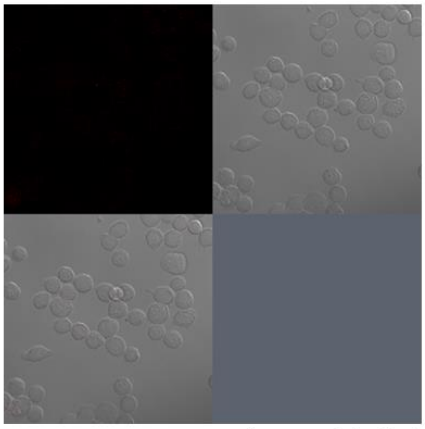

MDA-MB-453 + 1uM Alexa555-labeled WT-FN3, 30min on ice

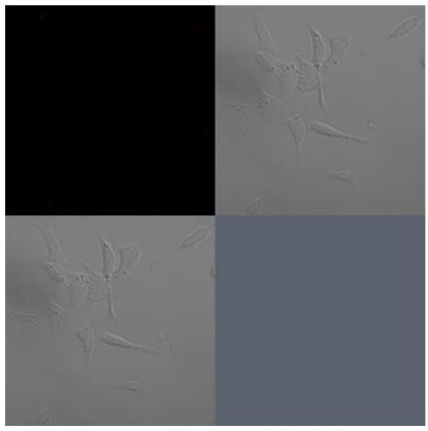

SKOV3 + 1uM Alexa555-labeled WT-FN3, 30min on ice

CHAPTER 3

Generation and characterization of a biparatopic ErbB3-targeting SDA^{HER3}

Introduction

Cancer is a complex disease, which usually involves multi-factors during the development and progression. Bispecific antibodies draw attention in the field of immunotherapy and oncology. The major interests in bispecific antibodies are to combine two fragments from two different monoclonal antibodies that bind to different antigens. Although it is indeed interesting in engineering a bispecific SDA, in the present study, we focused on developing biparatopic agent that targeting solely against ErbB3. There were a few studies indicated the advantages of biparatopic antibodies/proteins targeting other members of ErbB family or other receptors[61–64]. Roovers and his colleagues combined two anti-EGFR nanobodies that improve the efficacy and potently inhibited the EGF-depend cell proliferation[64]. Li from MedImmune demonstrated an biparatopic ErbB2-targeting antibody-drug conjugate having therapeutic effect in T-DM1 eligible, resistant and ineligible patients during pre-clinical trials[61].

As introduced in the first chapter, the currently ErbB3 antibodies under development has three major mechanism of actions, targeting the NRG1 binding, disrupting the dimerization between other ErbB receptors, or inducing the degradation of ErbB3[37]. In our study, the selected two SDAs from two selections have distinct

sequences, as well as slightly different binding affinities. Therefore, it was suspected that the two SDAs, SDA^{HER3}-A1 and SDA^{HER3}-D5, bind to the extracellular domain of ErbB3 at different sites. Moreover, the solubility and stability of SDA^{HER3}-D5 was not as good as that of SDA^{HER3}-A1. In order to improve the biophysical properties of the selected SDAs, and take the advantage of the biparatopic agent, SDA^{HER3}-A1 and SDA^{HER3}-D5 were linked together by a flexible linker. The new biparatopic SDA^{HER3} was constructed, expressed and purified. The biochemical characteristics and cellular effects of the new agent were also tested.

Materials and Methods

Construction, expression and purification of SDA^{HER3}-D5A1 and SDA^{HER3}-D5A1-Cys

The coding gene of SDA^{HER3}-D5A1 was optimized first. The plasmid for SDA^{HER3}-D5A1-Cys was synthesized by Genescript. The plasmid was transformed to *E.coli* DH5α (New England BioLabs) and amplified. Part of the extracted plasmid was transformed to *E.coli* BL21 (DE3) competent cells (New England BioLabs) for protein expression. The other part of the plasmid was digested with Nco I & Sal I (New England BioLabs) and ligated to digested pET28b plasmid (by Nco I & Xho I, New England BioLabs). The ligated plasmid was confirmed by DNA sequencing (Eton BioScience) and transformed to *E.coli* BL21 (DE3) competent cells (New England BioLabs) as well. Cells were grown in LB media with kanamycin at 37 °C until OD ~0.6 (600 nm) and then induced with 0.3 mM IPTG at 20 °C for 16 h. The purification process was performed as above.

Affinity determination and specificity by Bio-Layer Interferometry (BLI) analysis

The binding affinity and specificity of SDA^{HER3}-D5A1 was determined on an Octet RED384 instrument (Pall Fortbio, UNC Macromolecular Interactions Facility). All measurements were ran at 30 °C with black 96-well microplates (Greiner Bio-One). Anti-human IgG Fc Capture (AHC) biosensors (Pall Fortbio) were used for measurements. Human EGFR ECD-Fc, ErbB2 ECD-Fc, ErbB3 ECD-Fc and ErbB4 ECD-Fc (R&D Systems) were dissolved in the running buffer (1 x PBS, 0.002% Tween 20, pH 7.4). Receptors were immobilized to the biosensors with a concentration of 5ug/well. The concentration of the SDAs varied according to different types of proteins in different experiments. The data were obtained by data acquisition software from

forteBio. The acquired data was further processed and analyzed by data analysis software from forteBio. All the binding curves were performed by a 2:1 hetero- binding model.

Labeling SDA^{HER3}-D5A1 for cellular binding

For protein labeling, SDA^{HER3}-D5A1-Cys was used to react with Alexa-Fluor 555 C2 maleimide (Life technologies) following the steps as described previously. SDA^{HER3}-D5A1 was reacted with Cyanine5.5 NHS ester (Lumiprobe), with the same steps as described previously for SDAs reacting with Alexa-Fluor 555 carboxylic acid. All the labeled proteins were further purified with NAP-5 column (GE healthcare) to remove excess fluorescent dyes.

Cell culture

ErbB3-positive MDA-MB-453, MCF7, BT474 and ErbB3-negative MDA-MB-231, SKOV3, PANC1 were obtained from UNC Tissue Culture Facility. Each cell line was cultured by serial passage with proper media in 5% CO_2 incubator, at 37 °C.

Confocal microscopy and competition study

The binding test of SDA^{HER3}-D5A1 was performed similar to what has been described above, except the incubation was 30 min at room temperature. For competition experiments, the unlabeled SDA^{HER3}-A1, SDA^{HER3}-D5 and SDA^{HER3}-D5A1 were pre-mixed with Alexa-Fluor 555-labled SDA^{HER3}-D5A1-Cys in a ratio of 10:1 (2μM:200nM) before incubating with cells. The sample preparation was the same as previously described. All samples were examined with Zeiss LSM 700 confocal microscopy at UNC Microscopy Services Laboratory (MSL).

Flow cytometry and cell-binding study

Cellar binding affinity of SDA^{HER3}-D5A1 was determined by flow cytometry. Approximately 3 x 10^4 cells were collected. The cells were washed with 1 x PBS first. One set of cells were pre-blocked with 5 μM unlabeled SDA^{HER3}-D5A1 first for 30 minutes at 37 °C to get the non-specific binding signals. Then all cells were incubated with 0, 62.5, 125, 250, 500, 1000 nM SDA^{HER3}-D5A1-Cy5.5 samples on ice for 1 h, followed by 1 x PBS washing twice. The cells were fixed with 2% paraformaldehyde (PFA) for 15 min and washed by 1 x PBS once. The samples were analyzed by a flow cytometry (Cyan ADP analyzer, UNC flow cytometry core). Summit 4.4 (Beckman Coulter) and GraphPad Prism 6 was used for data analysis.

Cell proliferation assay

CellTiter 96 AQ_{ueous} one solution cell proliferation assay (Promega) was used for cell proliferation MTS assay. Approximately 5 x 10^4 cells were seeded in each (96 well plats) and grew overnight at 37 °C. The cells were starved with appropriate media containing 1% FBS for 24 hours at 37 °C. Different concentrations of SDA^{HER3}-D5A1 were incubated with cells for 48 hours at 37 °C. The MTS assay followed the manual provided by the manufacture and the absorbance at 485 nm was recorded using a HTS 7000 bioassay plate reader (PERKin Elmer). GraphPad Prism 6 was used for data analysis.

Result

Construction, expression and purification of SDA^{HER3}-D5A1 and SDA^{HER3}-D5A1-Cys

The genetic code for SDA^{HER3}-D5A1 was optimized for expression. The construction, expression and purification of SDA^{HER3}-D5A1 and SDA^{HER3}-D5A1-Cys were successful. The biparatopic SDA^{HER3}-D5A1 has increased level of expression, as well as with improved stability and solubility. The Figure 3.1 showed the purified products of SDA^{HER3}-D5A1 and SDA^{HER3}-D5A1-Cys on SDS-PAGE gel. The size of the two products were consistent with design and the purities were satisfying. The generated SDA^{HER3}-D5A1-Cys provided modification sites for conjugation and applications.

SDA^{HER3}-D5A1 binds to ErbB3 with picomolar affinity and specificity *in vitro*, and it selectively binds to ErbB3-positive cells

The biparatopic molecule usually has greater binding affinity than its components. It is consistent in our study. The generated SDA^{HER3}-D5A1 molecule has picomolar affinity (80.3 ± 20.3 pM) to ErbB3 whose binding affinity is about 10 x tighter than that SDA^{HER3}-A1 and 30 x than that of SDA^{HER3}-D5. The dissociation rate of SDA^{HER3}-D5A1 was very slow, as shown in Figure 3.2. Human EGFR ECD-Fc, ErbB2 ECD-Fc, ErbB3 ECD-Fc and ErbB4 ECD-Fc were used for specificity test (Figure 3.3). SDA^{HER3}-D5A1 did not bind to EGFR and ErbB2, however, it showed binding to ErbB4 besides ErbB3. Considering the fact that NRGs are the ligands for ErbB3 and ErbB4, it is reasonable that our SDA also has binding affinity to ErbB4. To confirm the binding and possible mechanism of SDA^{HER3}-D5A1 against ErbB4, the K_D was measured as

16.5±6.8 nM (Figure 3.4), which is almost 200 fold weaker than its binding to ErbB3. The binding of SDA^{HER3}-A1, SDA^{HER3}-D5 and SDA^{HER3}-D5A1 against ErbB4 with the same concentration was also tested as shown in Figure 3.5. The result supported the hypothesis that the binding of SDA^{HER3}-D5A1 against ErbB4 may related to the NRG1 binding sites since only SDA^{HER3}-D5 that may compete with NRG1. However, the binding affinity of the SDA^{HER3}-D5A1 against ErbB4 is much higher than SDA^{HER3}-D5. Overall, SDA^{HER3}-D5A1 selectively bind to the extracellular domain of ErbB3 with picomolar binding affinity *in vitro*.

The binding of SDA^{HER3}-D5A1 to ErbB3 receptors on cell surface was confirmed by confocal microscopy as shown in Figure 3.6. MDA-MB-453 is a breast cancer cell line with ErbB3 overexpressed and SKOV3 is an ovarian cancer cell line with no/minimum ErbB3 expression. The labeled SDA^{HER3}-D5A1 showed cellular binding when incubated with MDA-MB-453 cells and did not bind to SKOV3 cells. It suggested that SDA^{HER3}-D5A1 selectively bind to ErbB3 overexpressed cancer cells.

Competition assay supported that SDA^{HER3}-D5A1 is a biparatopic molecule and binds to ErbB3

The availability of SDA^{HER3}-D5A1 made it possible to check whether SDA^{HER3}-A1 and SDA^{HER3}-D5 bind to different sites on the extracellular domain of ErbB3. A competition test was performed with confocal microscopy. If the binding of SDA^{HER3}-A1 and SDA^{HER3}-D5 compete with each other, then either SDA^{HER3}-A1 or SDA^{HER3}-D5 is able to block the binding of labeled SDA^{HER3}-D5A1. As shown in Figure 3.7, with 30 min incubation at room temperature, the confocal data clearly demonstrated the binding of 200 nM labeled SDA^{HER3}-D5A1 to the ErbB3-positive MCF7 cells. A 10 x concentrated

unlabeled SDA^{HER3}-D5A1 was used as a positive control. After being mixed together with labeled SDA^{HER3}-D5A1, and the binding of labeled SDA^{HER3}-D5A1 was totally blocked. However, when mixed with 10 x concentrated SDA^{HER3}-A1 or SDA^{HER3}-D5, the labeled SDA^{HER3}-D5A1 still showed cellular binding to MCF7 cells. Only when mixing with 10 x concentrated SDA^{HER3}-A1 and SDA^{HER3}-D5 together, the binding of labeled SDA^{HER3}-D5A1 was then attenuated. The results implied that SDA^{HER3}-A1 and SDA^{HER3}-D5 did not compete with each other when binding to ErbB3, and the new SDA^{HER3}-D5A1 molecule is indeed a biparatopic molecule.

Cellular binding affinity of SDA^{HER3}-D5A1 to ErbB3-positive cell line

The cellular binding affinity of SDA^{HER3}-D5A1 was determined by flow cytometry. Cells were pre-blocked with 5 μM SDA^{HER3}-D5A1 to induce the internalization of the surface ErbB3 receptors. Therefore, the results from the pre-blocked samples can be considered as the non-specific binding. After the subtraction the background and normalization, the data was fitted by the one-site specific binding in GraphPad Prism. The K_D of SDA^{HER3}-D5A1 to ErbB3-positive MCF7 cells is 35.61 ± 17.07 nM. For ErbB3-negative PANC1 cells, the fitting curve for SDA^{HER3}-D5A1 did not converge, and the binding signal before normalization was much smaller than that with MCF7 cells. The result suggested that SDA^{HER3}-D5A1 selectively binds to ErbB3-positive cells with ~30 nM cellular binding affinity.

SDA^{HER3}-D5A1 inhibited the NRG1 induced proliferation

MTS assay was used to determine whether SDA^{HER3}-D5A1 has any effect on cell proliferation. Sheng and his colleagues proposed the important role of NRG/ErbB3 autocrine loop[65]. The autocrine ligand-receptor stimulates growth stimulation and

tumorigenesis in cancers[45]. Two ErbB3-positive breast cancer cells, MCF7 and BT474, as well as ErbB3-negative MDA-MB-231 cells, were used to perform the proliferation assay. The SDA^{HER3}-D5A1 did not show any inhibition effect on any of the cell lines alone (as shown in Figure 3.9 for BT474 cell line). However, after the stimulation by 10 nM NRG1, SDA^{HER3}-D5A1 inhibited the ligand-induced proliferation of MCF7 and BT474. Different concentrations of SDA^{HER3}-D5A1 were applied and the results showed a dose-dependent inhibition effect. To calculate the growth inhibition, the readings from stimulated cells were subtracted by the readings from unstimulated ones according to different treatments. The final readings were normalized and fitted by (logged) concentration vs. normalized response curves. The EC_{50} of the inhibition to the ligand-induced proliferation are 52.72 ± 12.44 nM and 178.8 ± 64.7 nM with SDA^{HER3}-D5A1 for BT474 and MCF7 cells, respectively, as shown in Figure 3.10. The ErbB3-negative PANC1 cells did not stimulated by NRG1, thus the SDA^{HER3}-D5A1 showed no inhibition effect. In all, SDA^{HER3}-D5A1 did not inhibit the normal cancer cell growth; however, it inhibits the NRG1-induced cell proliferation in cancers that are ErbB3-driven or through ErbB2-ErbB3 dimerization. SDA^{HER3}-D5A1 may be a good candidate for cancer treatment or in combination with other therapeutic agents.

Discussion

In the present study, we constructed a biparatopic molecule SDA^{HER3}-D5A1 that targets the extracellular domain of ErbB3 from SDA^{HER3}-A1 and SDA^{HER3}-D5. SDA^{HER3}-D5A1 has an improved level of expression, solubility and stability. Similar to the biparatopic anti-VEGFR nanobody reported by Fleetwood and his colleagues[62], the generated SDA^{HER3}-D5A1 has picomolar binding affinity to ErbB3 with specificity *in vitro*, which makes SDA^{HER3}-D5A1 a good candidate for further development. Cellular binding of SDA^{HER3}-D5A1 was confirmed by confocal microscopy and a K_D was determined by flow cytometry. SDA^{HER3}-D5A1 selectively binds to ErbB3-positive cell lines. However, the cellular binding affinity is much weaker than the binding affinity determined by Octet Red. It may due to the limitation of the fluorescence molecules or the flow cytometry machine. The enriched ErbB3 concentration on the surface of the anti-Fc sensors by immobilization may artificially increase the binding affinity. It is also because of the conjugation of the dye that effect the cellular binding affinity. The result from the competition assay by confocal microscopy supported the assumption that SDA^{HER3}-A1 and SDA^{HER3}-D5 bind to different site of ErbB3 and does not compete with each other, and the constructed SDA^{HER3}-D5A1 is indeed a biparatopic molecule. Once we confirmed the binding of SDA^{HER3}-D5A1, the next step was to evaluate the cellular effect of SDA^{HER3}-D5A1. Lee-Hoeflich and her colleagues explored the role of ErbB3 in ErbB2-amplified breast cancer. They discovered that the knockdown of ErbB3 inhibited the growth BT474 tumor and induced tumor regression[66]. In low ErbB2-expressing cancer cells such as MCF7, ErbB3 is also a key sensor in regulating ErbB-mediated signaling pathways[67]. Clinical studies with ErbB3-targeting antibody MM-121 has

already proved its usage in breast cancer patients with low-expression of ErbB2[68]. In the present study, PANC1 was used as a negative control for proliferation assay. No stimulation from PANC1 was observed. Thus, there is no inhibition effect from the addition of SDA^{HER3}-D5A1. BT474 is a cell line with overexpression of ErbB2 and ErbB3, while MCF7 has low expression of ErbB2. Both of the cell lines were stimulated by 10 nM NRG1. The result suggested that SDA^{HER3}-D5A1 has better (about three folds) inhibition effect to the ligand-induced proliferation in BT474 cells than MCF7 cells. It may imply that SDA^{HER3}-D5A1 is able to disrupt the dimerization of ErbB2-ErbB3, which contributes to the improved inhibition effect in BT474 cells. Lazrek and his colleagues reported a combination of anti-ErbB3 domain I and III antibodies effectively inhibited tumor growth by disrupting the dimerization and Akt induced downstream signaling pathways[69], which is consistent with our result. Therefore, it is possible that our biparatopic SDA^{HER3}-D5A1 has similar mechanisms in inhibition ligand-induced proliferation. Overall, SDA^{HER3}-D5A1 has potentials to be a therapeutic agent targeting ErbB3-overexpressed cancer cells.

Figure 3.1 Purification of SDA^{HER3}-D5A1 and SDA^{HER3}-D5A1-Cys

SDS-PAGE (12%) of the purified SDA^{HER3}-D5A1 and SDA^{HER3}-D5A1-Cys by Ni-NTA resin. The SDA^{HER3}-D5A1 was a monomer with a size ~30 kDa while SDA^{HER3}-D5A1-Cys was a mixture of monomer and dimer (~60 kDa). The cartoon illustrated the schematic and design of SDA^{HER3}-D5A1.

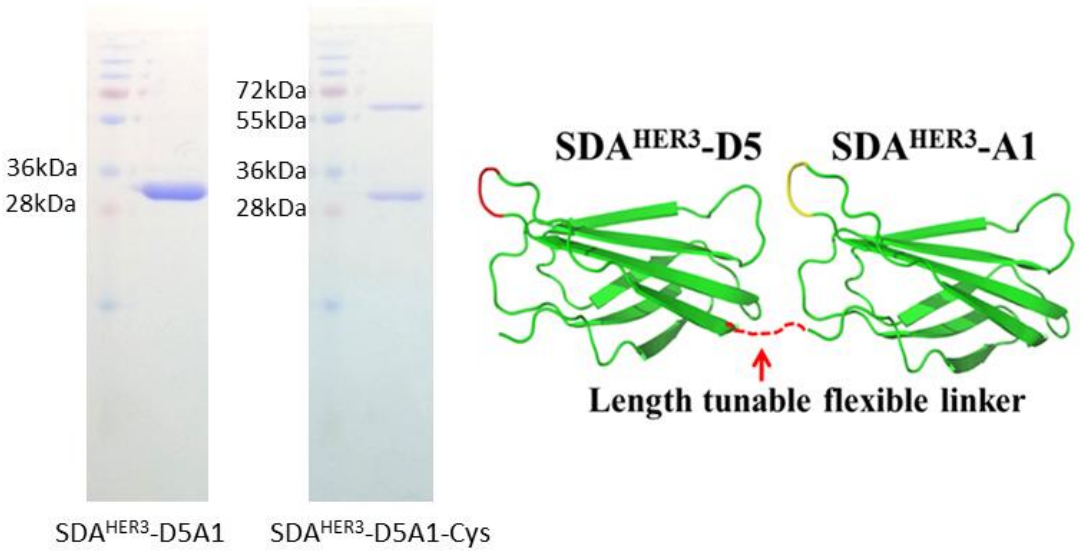

Figure 3.2 The binding affinity of SDA^{HER3}-D5A1 to ErbB3 ECD-Fc

Four different concentration (31.25 nM, 62.5 nM, 125 nM, 250 nM) of SDA^{HER3}-D5A1 were used in the binding experiment. Similar to SDA^{HER3}-A1 and SDA^{HER3}-D5, SDA^{HER3}-D5A1 has good on-rate. SDA^{HER3}-D5A1 has slower dissociation rate if compared to the parent SDAs. The calculated K_D for SDA^{HER3}-D5A1 to ErbB3 is 80.3 ± 20.3 pM, which increases ~ 10 fold binding affinity to that of SDA^{HER3}-A1.

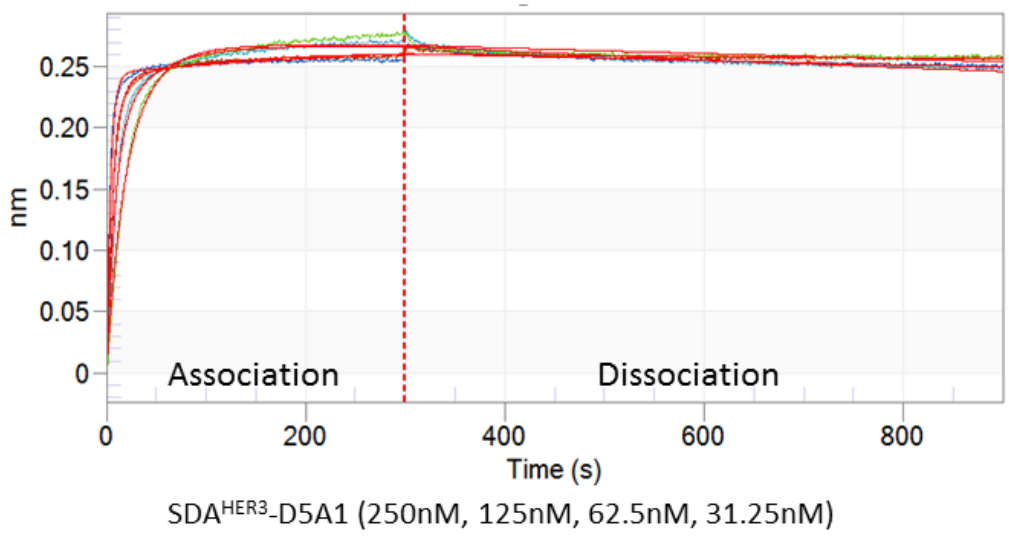

Figure 3.3 Selectivity of SDA^{HER3}-D5A1 to ErbB receptor family

Human EGFR ECD-Fc, ErbB2 ECD-Fc, ErbB3 ECD-Fc and ErbB4 ECD-Fc were immobilized to anti-Fc sensors. 500 nM of SDA^{HER3}-D5A1 was used to test whether SDA^{HER3}-D5A1 binds to the ErbB receptors. SDA^{HER3}-D5A1 showed no/minimum binding to the extracellular domain of EGFR and ErbB2. It showed binding to both ErbB3 and ErbB4 while it has much stronger binding affinity to ErbB3.

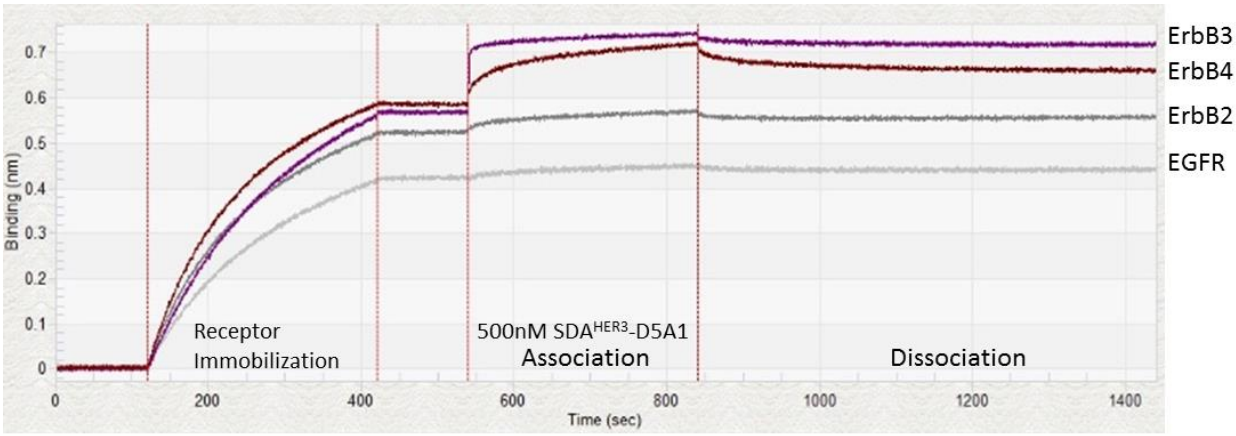

Figure 3.4 Binding affinity of SDA^{HER3}-D5A1 against ErbB4

The binding affinity of SDA^{HER3}-D5A1 against ErbB4 was determined as 16.5±6.8 nM. The association SDA^{HER3}-D5A1 to ErbB4 were much slower than that to ErbB3 and the dissociation of SDA^{HER3}-D5A1 to ErbB4 were much faster.

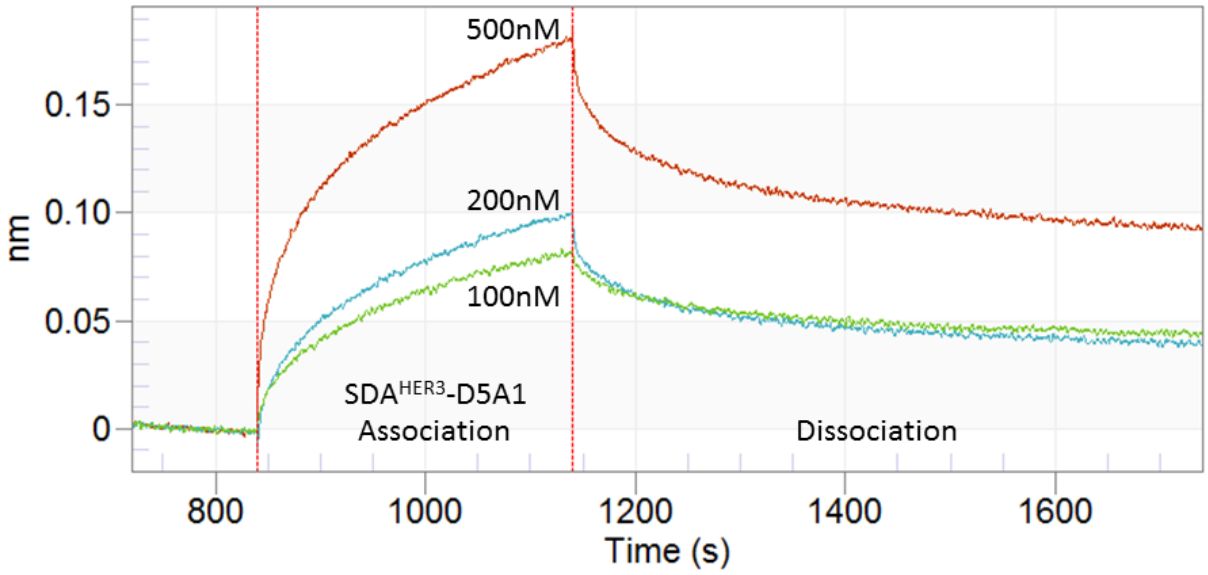

Figure 3.5 The binding curve of SDA^{HER3}-A1, SDA^{HER3}-D5 and SDA^{HER3}-D5A1 to the extracellular domain of ErbB4

To explore the potential binding mode of SDA^{HER3}-D5A1 against ErbB4, 500 nM of SDA^{HER3}-A1, SDA^{HER3}-D5 and SDA^{HER3}-D5A1 were used to get the binding curves to ErbB4. Interestingly, SDA^{HER3}-A1 does not bind to ErbB4 and SDA^{HER3}-D5 only has small response during the association. SDA^{HER3}-D5A1 itself has much stronger binding to ErbB4 than its parent subunits.

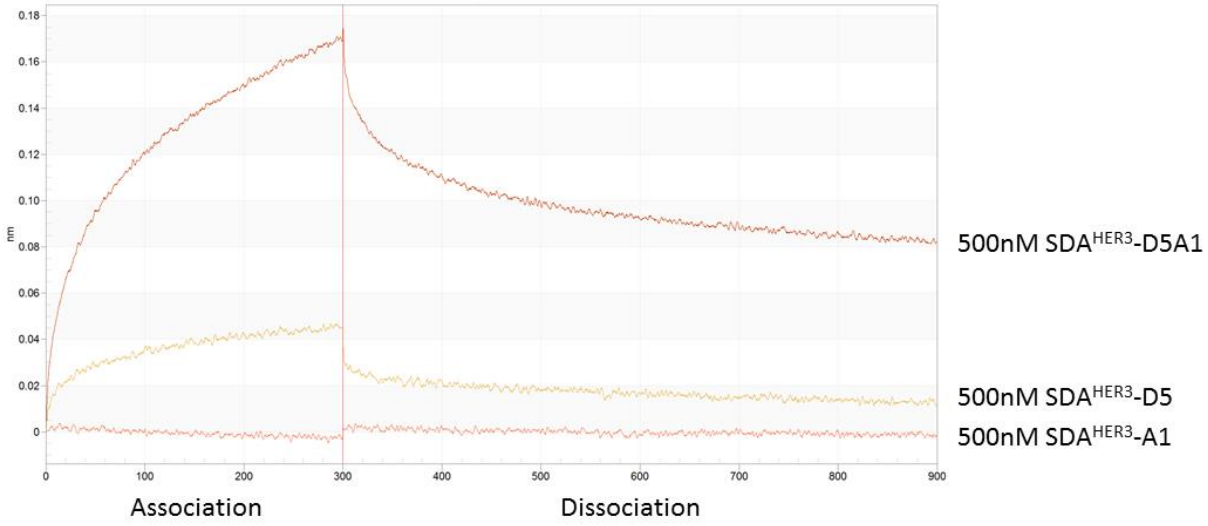

Figure 3.6 SDA^{HER3}-D5A1 selectively binds to ErbB3-positive cell line

The SDA^{HER3}-D5A1-Alexa-Fluor 555 showed binding to MDA-MB-453, a breast cancer cell line, with ErbB3 overexpressed; but the same molecule did not show binding to SKOV3, an ovarian cancer cell line with no/minimum ErbB3 expressed.

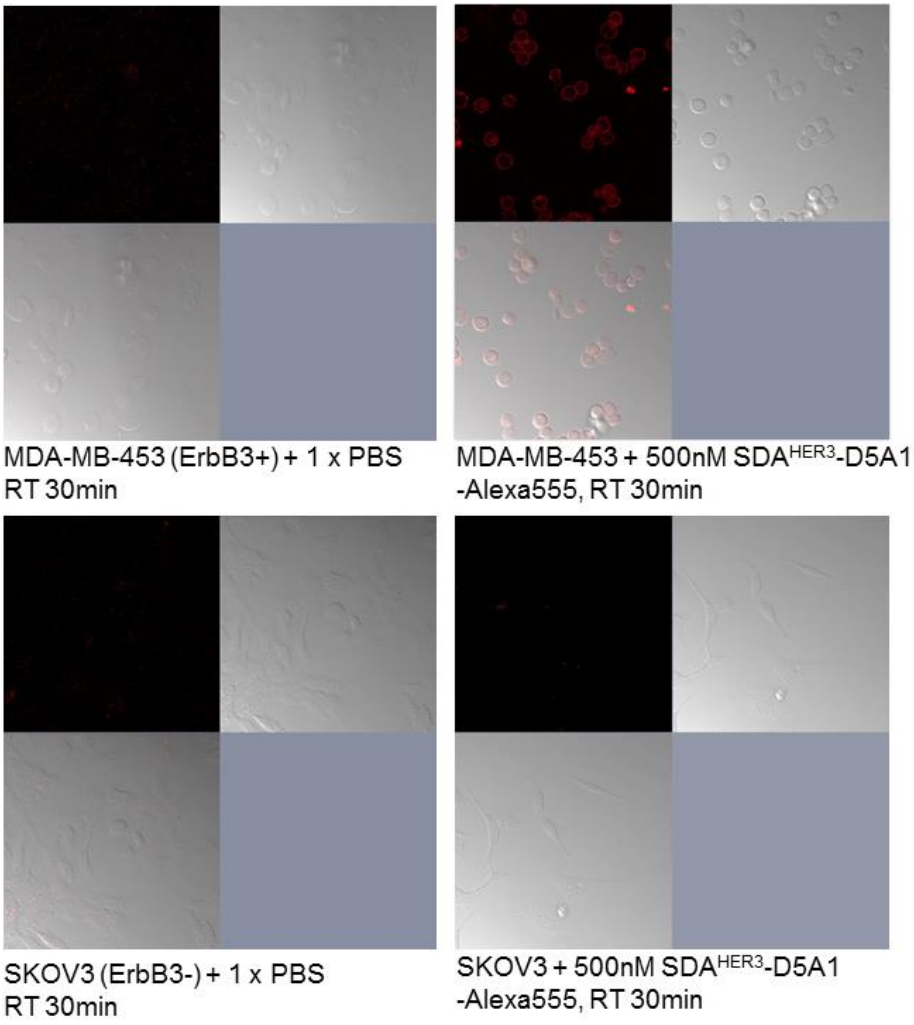

Figure 3.7 Competition experiment with confocal microscopy supported the hypothesis that SDA^{HER3}-D5A1 is biparatopic molecule

The competition assay confirmed that SDA^{HER3}-A1 and SDA^{HER3}-D5 bind to different locations on the extracellular domain of ErbB3, thus, SDA^{HER3}-D5A1 is a biparatopic molecule. Neither 10 x excess of unlabeled SDA^{HER3}-A1 nor SDA^{HER3}-D5 blocked the binding of SDA^{HER3}-D5A1. Only the presence of both SDA^{HER3}-A1 and SDA^{HER3}-D5, or SDA^{HER3}-D5A1 itself blocked the binding of the Alexa-Fluor 555 labeled SDA^{HER3}-D5A1.

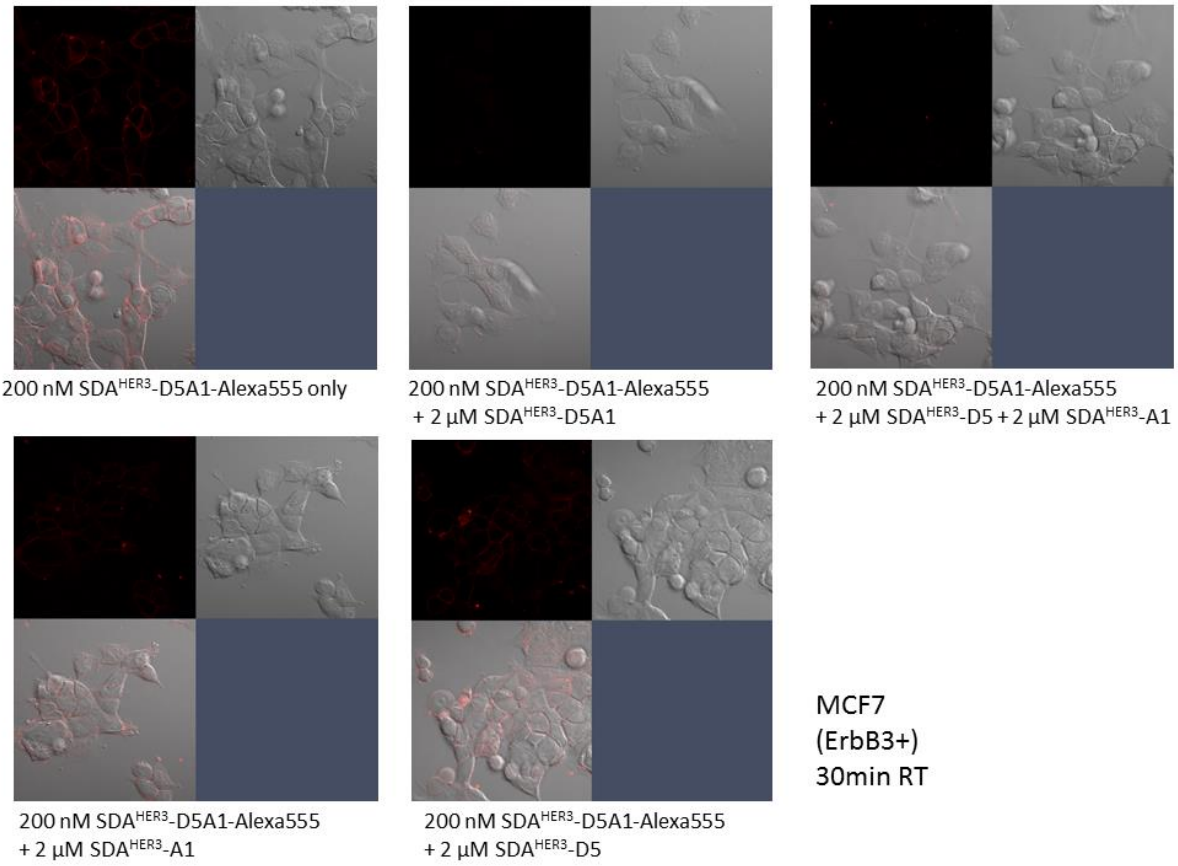

Figure 3.8 Flow Cytometry confirmed SDA^{HER3}-D5A1 selectively bind to ErbB3-positive cell line with good binding affinity.

The binding affinity of Cy5.5 labeled SDA^{HER3}-D5A1 to ErbB3-positive MCF7 is 35.61 ± 17.07 nM. The same molecule did not show concentrated dependent binding to PANC1 cells and the values of MFI were very small (data not shown).

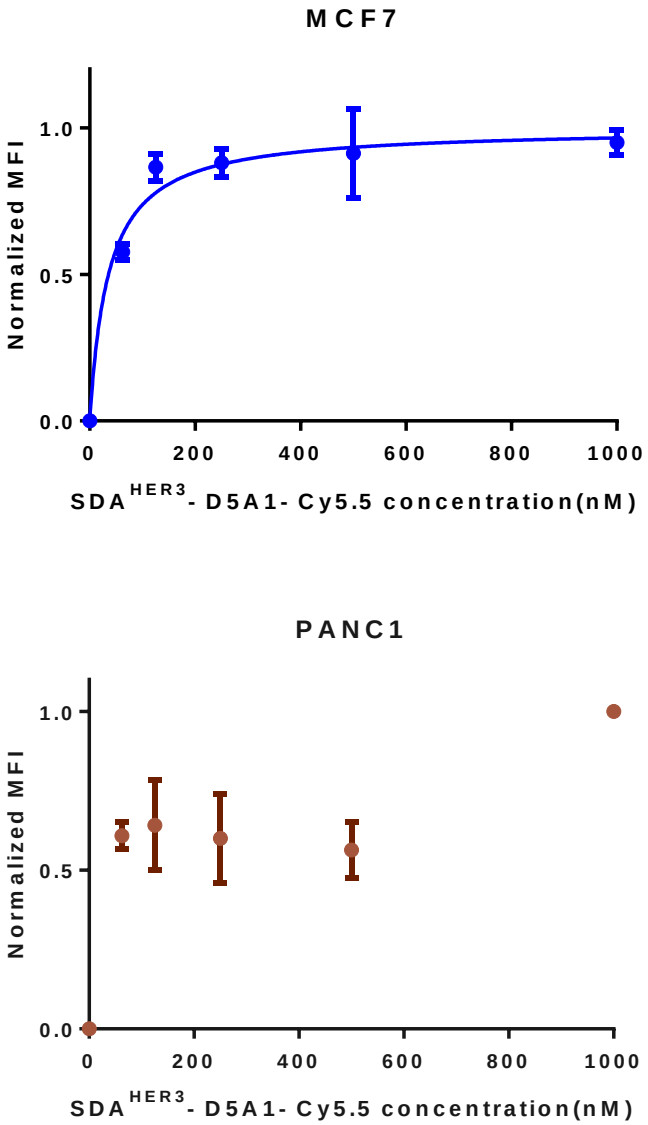

Figure 3.9 SDA^{HER3}-D5A1 does not stimulate or inhibit the normal cell growth while it inhibits the NRG1 stimulated cell proliferation

Different concentrations of SDA^{HER3}-D5A1 were applied to the BT474 cells and incubated for 48 hours. The protein did not stimulate or inhibit the cell growth of BT474 cells without the stimulation of NRG1. However, with the stimulation from NRG1, SDA^{HER3}-D5A1 showed a dose-dependent inhibition to the NGR1 stimulated cell proliferation.

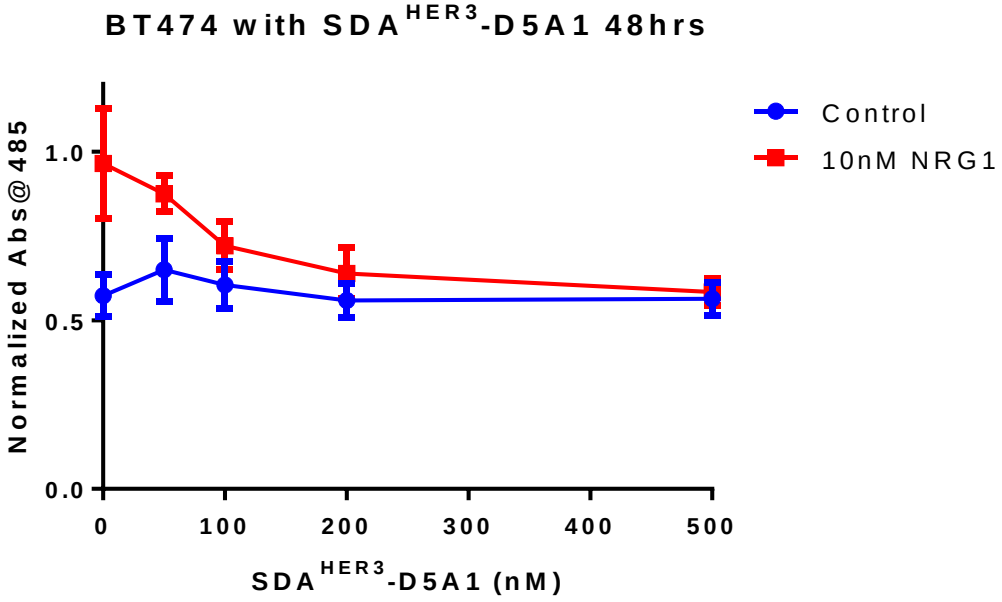

Figure 3.10 SDA^{HER3}-D5A1 showed growth inhibition to NRG1 stimulated proliferation for ErbB3-positive cell lines selectively

Different concentration of SDA^{HER3}-D5A1 were used to test the proliferation stimulated by 10 nM NRG1 of three different cancer cell lines, BT474 and MCF7 as ErbB3-positive cell lines, and PANC1 as ErbB3-negative cell line. The EC50 of the inhibition to the ligand-induced proliferation are 52.72 ± 12.44 nM and 178.8 ± 64.7 nM for BT474 and MCF7 cells, respectively. PANC1 did not stimulated by NRG1 and SDA^{HER3}-D5A1 showed no inhibition effect.

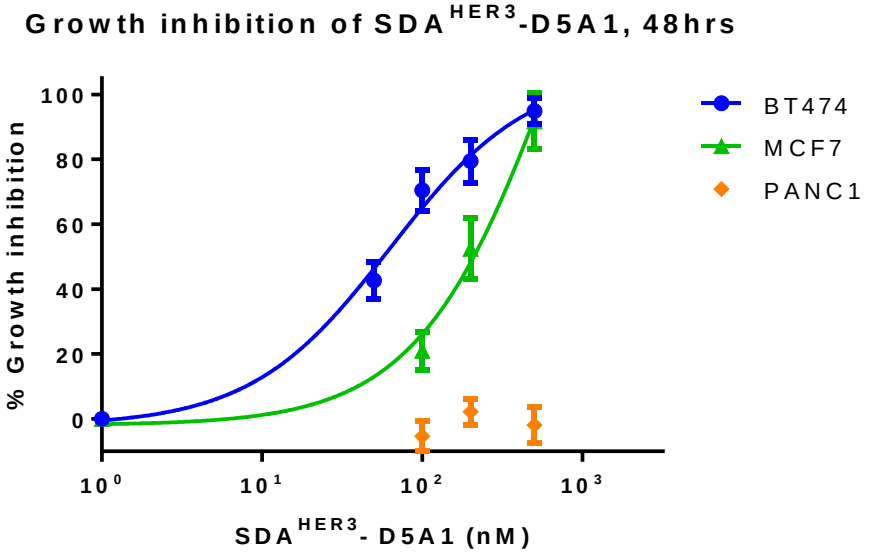

CHAPTER 4

Biparatopic ErbB3-targeting SDA^{HER3} as a theranostic agent

Introduction

Antibody-based drugs become a major new class of drugs in the recent years[70]. The mAbs with high affinity against important receptor targets have been proved very efficient and selective in clinical trials and treatments. Antibodies can be used as therapeutic agents, drug-delivery agents, or conjugated with imaging agents. It is well known that antibodies can be protein-based therapeutic agents for treatment. ADC with toxins[71] and targeted system for cancer therapy[72] attracts attentions in both academia and industry. Antibodies that targeting cell surface biomarkers can be used for molecular imaging of cancers as well[73]. For example, anti-ErbB2 antibody trastuzumab is among the first generation of antibody drugs. Originally, trastuzumab was used alone to treat late stage ErbB2-positive breast cancer[74]. A combination of trastuzumab with chemotherapy improved the survival and response rates[75]. Ado-trastuzumab emtansine is an antibody-drug conjugate of trastuzumab and a cytotoxic drug emtansine (DM1). It is used for treating patients with ErbB2-positive metastatic breast cancer and improves the progression-free and overall survival rate[76]. Other treatments includes combining trastuzumab with Lapatinib, or with pertuzumab and docetaxel, to improve the response and survival rates[29,77]. Besides the therapeutic effect from the monoclonal antibody and

ADC, trastuzumab was labeled with imaging agents such as IRDye800 and used for imaging purpose in mice xenograft models[78].

In most of the pre-clinical and clinical trials, the ErbB3 targeting antibodies were used as a combination of other agents for treatment[37]. ErbB3 is also a good candidate for targeted drug delivery[79]. Terwisscha van Scheltinga and Rosestedt presented their studies in utilizing ErbB3 targeting antibody and affibody in PET imaging, respectively[80,81]. In the present study, we performed some preliminary studies by utilizing the SDA^{HER3}-D5A1/ SDA^{HER3}-D5A1-Cys and different agents, including internalization and the delivery of gold nanoparticles, synergistic effect of applying SDA^{HER3}-D5A1 and Lapatinib together, and SDA^{HER3}-D5A1 with imaging agent in living mice.

Materials and Methods

Cell culture

ErbB3-positive ASPC1, MCF7, BT474 and ErbB3-negative MDA-MB-231, SKOV3, PANC1 were obtained from UNC Tissue Culture Facility. Each cell line was cultured by serial passage with proper media in 5% CO_2 incubator, at 37 °C.

Confocal microscopy and internalization assay

The SDA^{HER3}-D5A1-Cys was conjugated with Alexa-Fluor 555 C2 maleimide as previously described. The internalization test of SDA^{HER3}-D5A1 was performed similar to what has been described above, except the incubation was 2 hours at 37 °C. The sample preparation was the same as previously described. All samples were examined with Zeiss LSM 700 confocal microscopy at UNC Microscopy Services Laboratory (MSL).

AuNPs-mediated hyperthermia treatment with cancer cells

The conjugation of SDA^{HER3}-D5A1-Cys with AuNPs followed the steps as described in the previous work[53]. The quantification was performed with Bradford Assay Reagent (Thermo Scientific). ErbB3-positive MCF7 and MDA-MB-231 cells were seeded on the glass coverslides. After the treatment[53], the cells were stained by LIVE/DEAD® Viability/Cytotoxicity Kit, for mammalian cells (Life Technologies). After washing by 1 x PBS 3 times and fixed, the samples were examined by Zeiss LSM 700 at UNC Microscopy Services Laboratory (MSL).

Cell proliferation assay

CellTiter 96 AQ_{ueous} one solution cell proliferation assay (Promega) was used for cell proliferation MTS assay. The procedure was the same as described in the previous

chapter. The Lapatinib (Sigma) was dissolved in DMSO. Different concentration and combination of SDA^{HER3}-D5A1 and Lapatinib was used according to the IC_{50} of Lapatinib (BT474 ~ 25 nM, MCF7 ~ 6 μM, MDA-MB-231 ~ 6 μM)[82–84] and incubated for 48 hours at 37°C. The MTS assay followed the manual provided by the manufacture and the absorbance at 485 nm was recorded using a HTS 7000 bioassay plate reader (PERKin Elmer). GraphPad Prism 6 was used for data analysis.

Western blot analysis

Cells were seeded to 6 well plates and grew overnight. Cells were starved for 24 hours with media containing 1% FBS. Cells were stimulated with 10 nM NRG1 and different combinations of agents (200 nM SDA^{HER3}-D5A1, 2 μM Lapatinib) for 10 minutes. Cell lysates were quantified by DC Protein Assay (Bio-Rad) and separated by 12% SDS-PAGE gel. After transferred to the membrane, the corresponding strips were cut and incubated with antibodies, including phosphor-HER3/ErbB3 (21D3) Rabbit mAb (Cell Signaling), HER3/ErbB3 (1B2E) Rabbit mAb (Cell Signaling), phosphor-Akt (Ser473) XP Rabbit mAb (Cell Signaling), Akt(pan) (C67E7) Rabbit mAb (Cell Signaling), Phospho-p44/42 MAPK (ERK1/2) (Thr202/Tyr204) Rabbit mAb (Cell Signaling), p44/42 MAPK (ERK1/2) (137F5) Rabbit mAb (Cell Signaling), respectively, in a ratio of 1:2500 for 16 hours at 4 °C. ECL anti-rabbit IgG (GE healthcare) was used as secondary antibody.

Synthesis of IRDye 800-SDA^{HER3}-D5A1 and imaging study

Synthesis of SDA^{HER3}-D5A1-Cys and IRDye800CW Maleimide (LI-COR biosciences) followed the same steps as described in the previous section for thio-reactive dye with SDA^{HER3}-D5A1. The efficiency of the conjugation was determined by

NanoDrop 1000 (Thermo Fisher Scientific). The excessive dye was removed by NAP-5 column (GE healthcare).

A total of fifteen 4-6 weeks BALB/c nude mice (obtained from UNC animal study facility) were used for the present study. For each mouse, 5 million cells were injected to the shoulder. Ten mice were injected with ErbB3-positive ASPC1 cells and five mice were injected with ErbB3-negative PANC1 cells. After the tumor grew to a size of 200-500 cm^3, the mice were injected with labeled agents for imaging purpose. Mice anesthesia was conducted with 2-5% isoflurane in oxygen with a flow rate of 2L/min. Each mice was injected with 100 µL labeled agents. The time points for imaging were 1 hour, 4 hours, 12 hours and 24 hours. IVIS Kinetic (Caliper Life Sciences) was used to acquire quantitative fluorescence signals. The emission filter was ND3, and the excitation filter was 745. The result was analyzed by Living image software and the data was processed with GraphPad Prism.

Result

SDA^{HER3}-D5A1 got internalized and selectively targeted ErbB3-positive cells in hyperthermia treatment.

In the previous section, we confirmed the binding of SDA^{HER3}-D5A1 to the receptor ErbB3 on the surface of cancer cells. In this experiment, as shown in Figure 4.1, at 37 °C for 2 hours, the labeled SDA^{HER3}-D5A1 entered the cells. To validate the targeting effect of SDA^{HER3}-D5A1, SDA^{HER3}-D5A1-Cys was conjugated with gold nanoparticles and used for hyperthermia treatment. The result in Figure 4.2 illustrated that the SDA^{HER3}-D5A1-AuNP was selectively delivered into the ErbB3-positive MCF7 cells. With laser irradiation, the cancer cells were killed by the heating effect from the internalized AuNPs. However, using SDA^{HER3}-D5A1-AuNP did not have toxicity to the cells, and SDA^{HER3}-D5A1-AuNP did not target ErbB3-negative cells. Moreover, the AuNP without targeting ligands did not internalized into the normal cells. Therefore, SDA^{HER3}-D5A1-AuNP showed improved targeting efficiency of biomaterials and demonstrated biomarker-dependent killing effect to cancer cells.

A combination of SDA^{HER3}-D5A1 and Lapatinib showed improved inhibition efficiency in proliferation assay with ErbB2 and ErbB3 overexpressed cells

In the previous chapter, SDA^{HER3}-D5A1 demonstrated its inhibition effect on ligand-induced proliferation. Additional proliferation assays were performed to explore its synergistic effect with Lapatinib, an EGFR/ErbB2 TKI, on ErbB3-overexpressed cells. MCF7 is a cell line with overexpressed ErbB3 but low expression of ErbB2. BT474 is a cell line with both ErbB2 and ErbB3 overexpressed. MDA-MB-231 is a triple negative breast cancer cell line with low/minimum expression of ErbB3. Although both MCF7 and

MDA-MB-231 have some EGFR expressed[85] on the cell surface, they are not very sensitive to Lapatinib[83,84]; In contrast, Lapatinib efficiently inhibits the proliferation of BT474. The results were described in Figure 4.3 for MCF7 cell line, Figure 4.4 for BT474 cell line, and Figure 4.5 for MDA-MB-231 cells. Overall, when adding Lapatinib with a concentration near the IC_{50} value, the drug itself did not effectively inhibit the proliferation, but a combination of SDA^{HER3}-D5A1 and Lapatinib further inhibit the cell proliferation in ErbB2 and ErbB3-positive cell line (BT474) as an addition effect, which is consistent with the result from the previous chapter. However, it did not show effect with statistical significance with MCF7 cells. Therefore, it may be useful in developing combination therapy with Lapatinib in treating ErbB2 and ErbB3-positive cancers.

SDA^{HER3}-D5A1 inhibited the ligand-induced activation of the downstream pathways

PI3K/Akt and MAPK/ERK pathways are important downstream pathways of ErbB3 and the whole ErbB family. To check the activation and inhibition of the downstream pathways, the phosphorylation of ErbB3, Akt and ERK1/2 was checked by western blot analysis, as shown in Figure 4.6. The result suggested that the addition of SDA^{HER3}-D5A1 alone did not influence the downstream pathways. After adding 10 nM NRG1, the cells were stimulated and the elevated levels of phosphorylation were observed for ErbB3, Akt and ERK. Since Lapatinib is kinase inhibitors and it could not inhibit ErbB3, the addition of the drug only showed minor effect on Akt and ERK, possibly by targeting EGFR. Applying 200 nM SDA^{HER3}-D5A1 partially inhibited the phosphorylation of all three targets. A combination treatment of 200 nM SDA^{HER3}-D5A1 and 2 μM Lapatinib further inhibit the ligand induced phosphorylation of Akt and ERK. It

may explain the synergistic effect observed in the proliferation assay as mentioned above.

SDA^{HER3}-D5A1-IRDye800 conjugate as fluorescence imaging probe for ErbB3-expressing cancers

SDA^{HER3}-D5A1-IRDye800 was conjugated, purified and quantified before injecting to the ASPC1 or PANC1 mouse xenograft mice. Non-blocking and blocking of unlabeled SDA^{HER3}-D5A1 were used to eliminate the signals from non-specific binding. In ErbB3 expression ASPC1 tumors, SDA^{HER3}-D5A1-IRDye800 showed an increase in tumor:muscle ratio during the time course in the experiment. It may due to the accumulation in the circulation after injection. After the blocking, the fluorescence signal decreased a lot. On the other hand, a blocking treatment did not decrease the fluorescence signal, and the tumor:muscle ratio did not increase in PANC1 mouse xenograft model. The result suggested that SDA^{HER3}-D5A1-IRDye800 targeted the ASPC1 tumors in mice. The conjugated molecule may be useful for imaging purpose.

Discussion

Although the results listed in this chapter are mostly from preliminary data, all the experiments showed promising results in translate SDA^{HER3}-D5A1 into theranostic applications. Targeted delivery with nanoparticles may be useful in reducing the cytotoxicity and overcome the drug resistance[72,86]. Such proof of concept can be easily validated by conjugating the targeting ligand with gold nanoparticles and use nanoparticle-mediated hyperthermia for cancer treatment[87]. A similar work was presented by the previous work from our lab[53]. SDA^{HER3}-D5A1 is able to carry the conjugated nanoparticles and selectively target the ErbB3-expressing cells. It is possible to expand this application to many other targeted nanoparticle delivery systems with toxins or other therapeutic agents[72]. Many of the ErbB3 targeting antibodies in clinical trials are used together with other antibodies or small molecule drugs[37]. Thus, Lapatinib was selected to treat cancer cells together with SDA^{HER3}-D5A1. As expected, treatment of a combination of the two agents demonstrated better inhibition effect than using the agents separately in the ErbB2 and ErbB3 positive cell line. The western blot analysis helped understand the mechanism of the inhibition. SDA^{HER3}-D5A1 is able to inhibit the ligand-induced activation of the downstream pathways, including the phosphorylation of ErbB3, Akt and ERK by binding to the extracellular domain of ErbB3. Lapatinib can only partially inhibit the activation of Akt and ERK through inhibiting the kinase activity of EGFR and ErbB2. Thus, a combination of the two agents showed a addition effect towards the proliferation of the cancer cells, especially to those with both ErbB2 and ErbB3 overexpressed. The next step would be using mouse xenograft models to test whether SDA^{HER3}-D5A1 and the combination therapy can induce tumor

regression as described in similar works with anti-ErbB3 antibodies[61,88]. In order to validate the binding ability of SDA^{HER3}-D5A1 in mouse xenograft models, as well as its potential in live animal imaging, SDA^{HER3}-D5A1 was conjugated with IRDye800CW. The result suggested that SDA^{HER3}-D5A1-IRDye800 conjugate targeted the ErbB3-overexpressed ASPC1 tumor and accumulated in tumor through the course of time. A blocking experiment with excessive amount of unlabeled SDA^{HER3}-D5A1 confirmed that non-specific binding did not contribute to the entire observed fluorescence signal. In contrast, PANC1 tumor did not have any similar properties as ASPC1 after the injection of the conjugate, and the blocking did not show any effect in decrease the fluorescence signals. However, PANC1 mouse xenograft models had a higher tumor:muscle ratio after injection. It may due to the vascular permeability of different tumors[89]. The fluorescence signals from IRDye800 may also be influenced by the tumor position, size and other factors. Thus, it is difficult to directly quantify and compare the imaging results among different mice and types of tumors. In some reported experiments, PET imaging was used with several of isotopes, such as (111)In[78], (89)Zr[80], (68)Ga[90] and $^{99m}Tc(CO)_3$[91], which provides more accurate results for quantification.

Figure 4.1 Internalization assay confirmed that SDA^{HER3}-D5A1 bound to ErbB3 receptors and got internalized after 2 hours incubation at 37 °C

The labeled SDA^{HER3}-D5A1 selectively binds to ErbB3-positive ASPC1 cells and after incubation at 37 °C for 2 hours, the labeled SDA^{HER3}-D5A1 internalized into the cells.

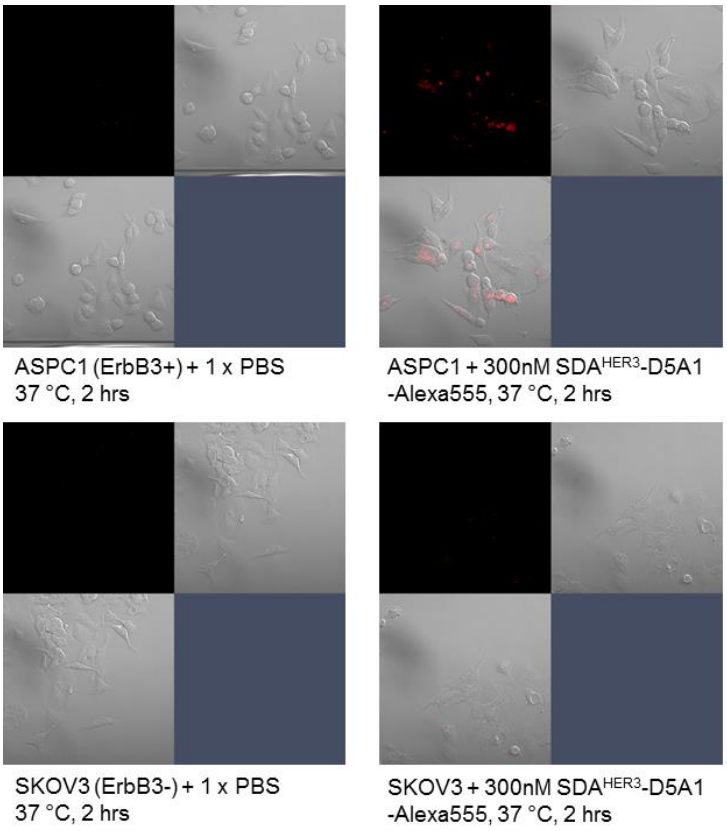

Figure 4.2 Hyperthermia treatment using SDA^{HER3}-D5A1-AuNP

The cells were incubated with 200 nM SDA^{HER3}-D5A1-AuNP at 37 °C for 2 hours to promote internalization. NIR laser (800 nm, 1W) was used for 8 minutes. Live/Dead cell staining kit was used to visualize living (green) and dead cells (red). Only ErbB3-positive MCF7 cells responded to hyperthermia treatment and cell death was observed near the center of the laser treatment.

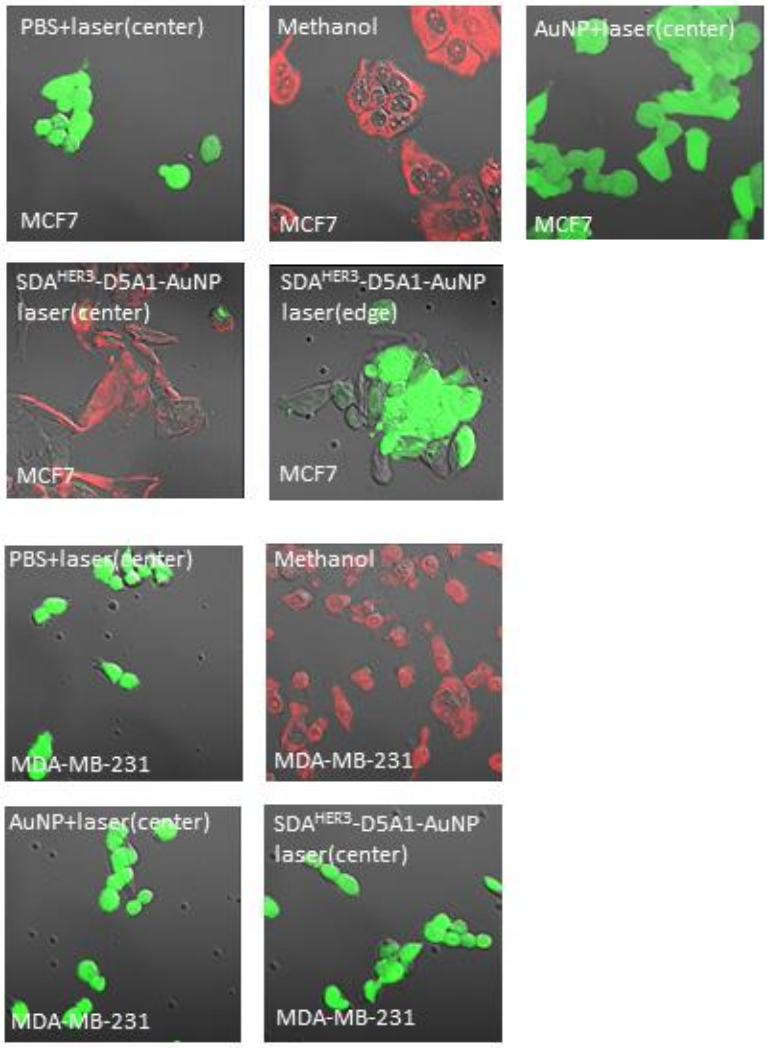

Figure 4.3 Proliferation of MCF7 cells, treated with 500 nM SDA^{HER3}-D5A1, 5 μM Lapatinib, and a combination of protein and the drug

MCF7 is an ErbB3-overexpressed cell line but with low expression of ErbB2. The addition of 500nM SDA^{HER3}-D5A1 inhibited the NRG1 stimulated proliferation. 5 μM Lapatinib did not inhibit the proliferation significantly. A combination of SDA^{HER3}-D5A1 and Lapatinib may show some further inhibition of the cell proliferation, however, the difference is not statistically significant.

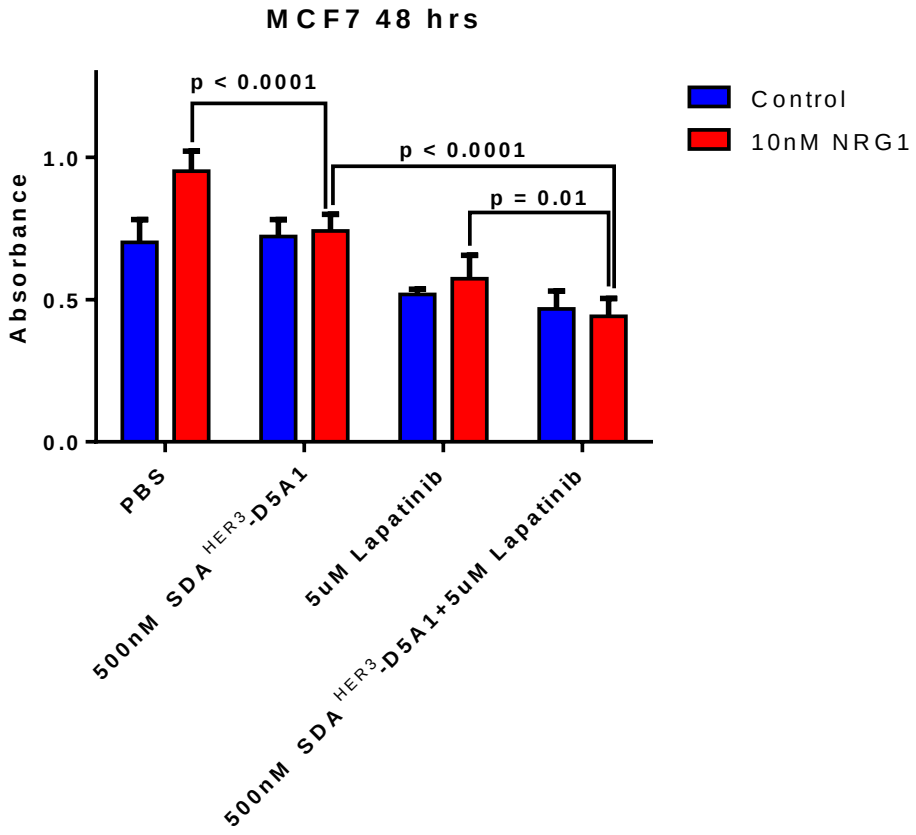

Figure 4.4 Proliferation of BT474 cells, treated with 500 nM SDA^{HER3}-D5A1, 5 μM Lapatinib (positive control), 25 nM Lapatinib and a combination of protein and the drug

BT474 is an ErbB2 and ErbB3-overexpressed cell line. The addition of 500nM SDA^{HER3}-D5A1 inhibited the NRG1 stimulated proliferation. 5 μM Lapatinib almost completely inhibit the growth of the cell. 25 nM Lapatinib did not show good inhibition to the ligand-induced proliferation, but in combination with SDA^{HER3}-D5A1, the inhibition effect was greatly improved.

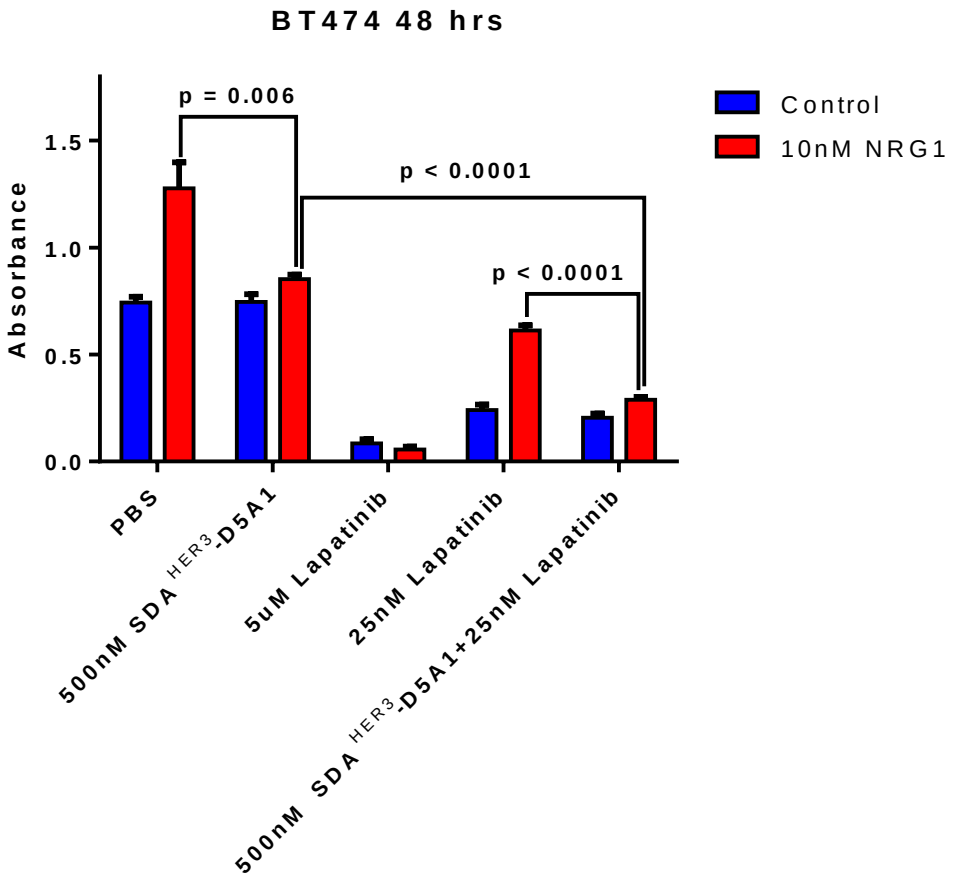

Figure 4.5 Proliferation of ErbB3-negative MDA-MB-231 cells, treated with 500 nM SDA^{HER3}-D5A1, 5 μM Lapatinib (positive control), 25 nM Lapatinib and a combination of protein and the drug

MDA-MB-231 is with no/minimum ErbB3 expression. It does not response to NRG1 stimulation and SDA^{HER3}-D5A1 showed on effect on proliferation. With 3 uM Lapatinib, the cell growth was slightly inhibited and an combination of the protein and drug did not show difference with significance.

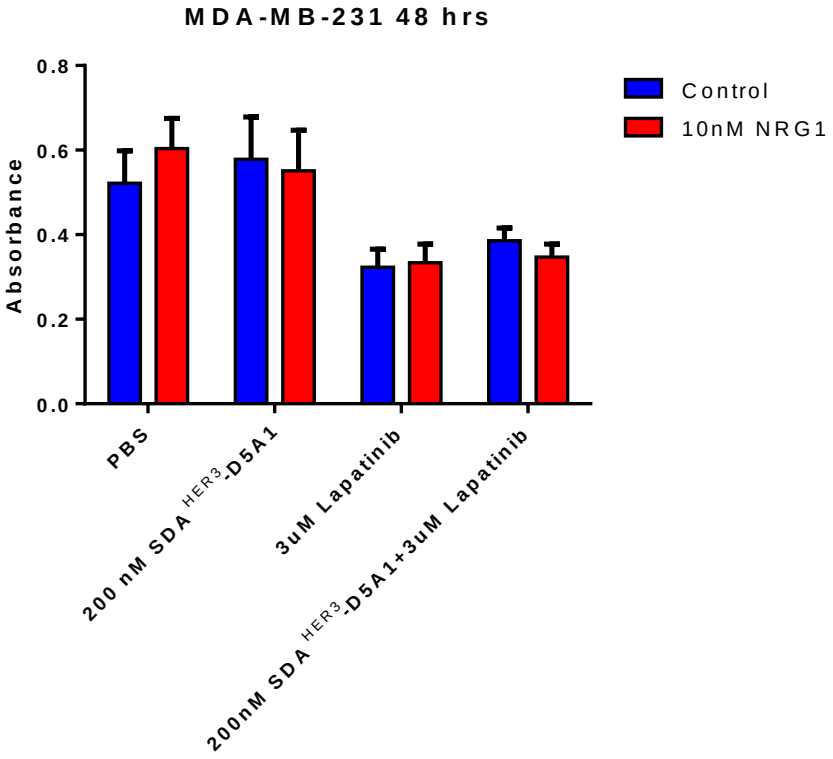

Figure 4.6 Western blot analysis of SDA^{HER3}-D5A1 and its effect on the downstream pathways of MCF7 cells

After 10 nM NRG1 stimulation, ErbB3, Akt and ERK were activated. Neither SDA^{HER3}-D5A1 nor Lapatinib could not inhibit phosphorylation of ErbB3, Akt and ERK by itself. However, a combination of the two demonstrated better inhibition effect on the NRG1-induced stimulation.

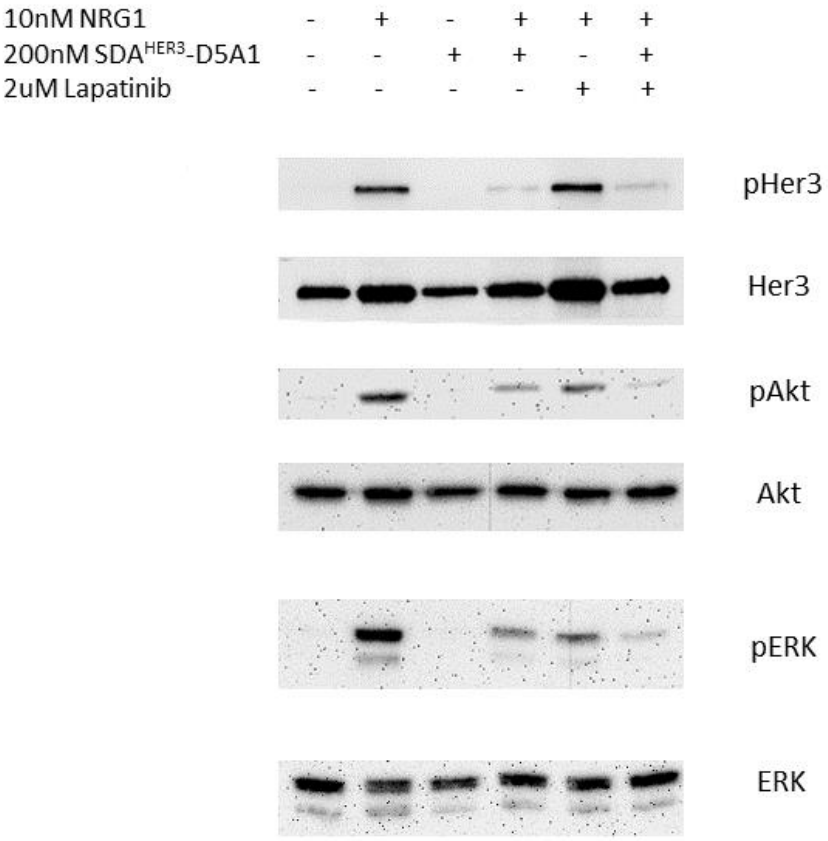

Figure 4.7 Live imaging results from ASPC1 mouse xenograft models with SDA^{HER3}-D5A1-IRDye800, for 1 hour, 4 hours and 24 hours after injection.

After injection, the major signals came from the tumor, liver and the kidney. The signals from the blood and tissues were gradually cleared. After 24 hours, the tumor region still maintained relatively high signals, which suggested the SDA^{HER3}-D5A1-IRDye800 bound to ASPC1 tumor.

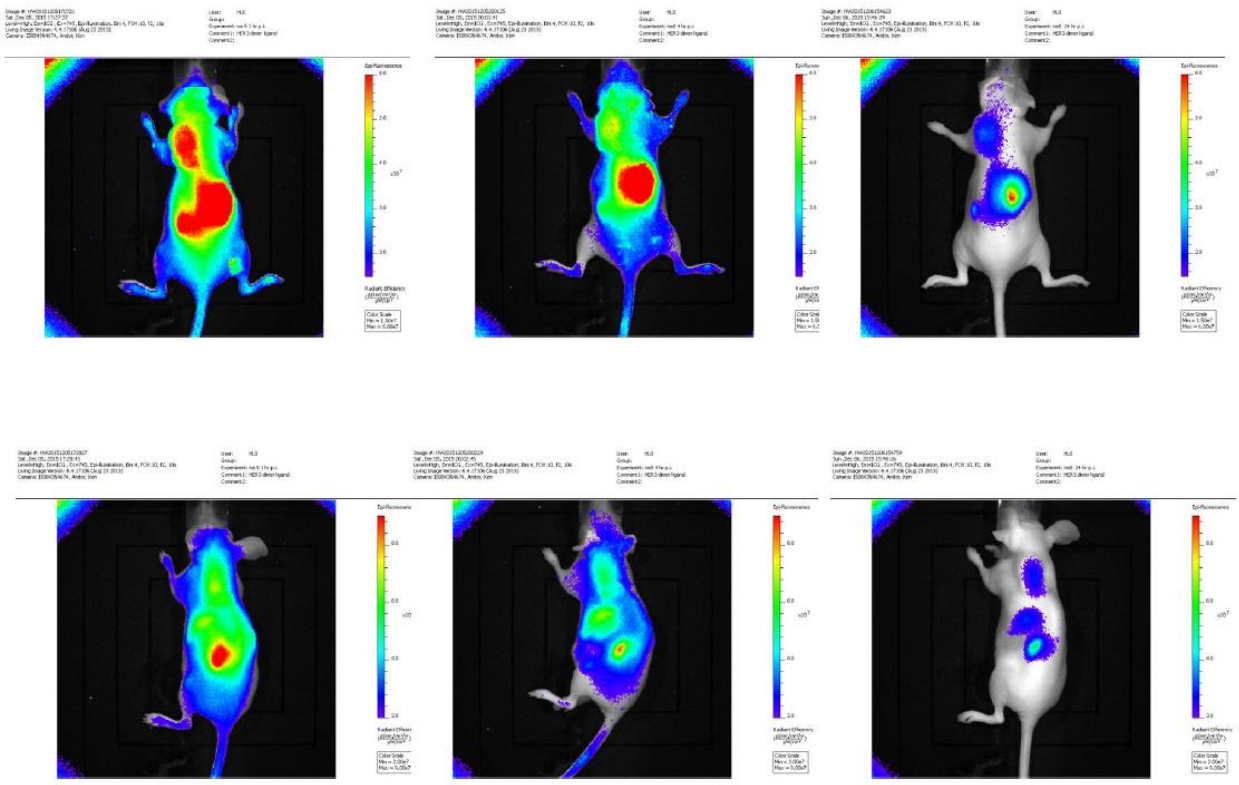

Figure 4.8 The change in tumor:muscle ratio after injection of SDA^{HER3}-D5A1-IRDye800 or SDA^{HER3}-D5A1-IRDye800 with 20 fold excess of unlabeled SDA^{HER3}-D5A1 (as blocking agent) at 1 hours, 4 hours, 24 hours and 48 hours in ASPC1 mouse xenograft model (Non-blocking: N = 7, Blocking: N =2)

The tumor:muscle ratio from the ASPC1 tumor increases over the time course. With blocking of unlabeled SDA^{HER3}-D5A1 proteins, the tumor:muscle ratio decreased significantly, which suggested the SDA^{HER3}-D5A1 bind to tumor with specificity in mouse xenograft models.

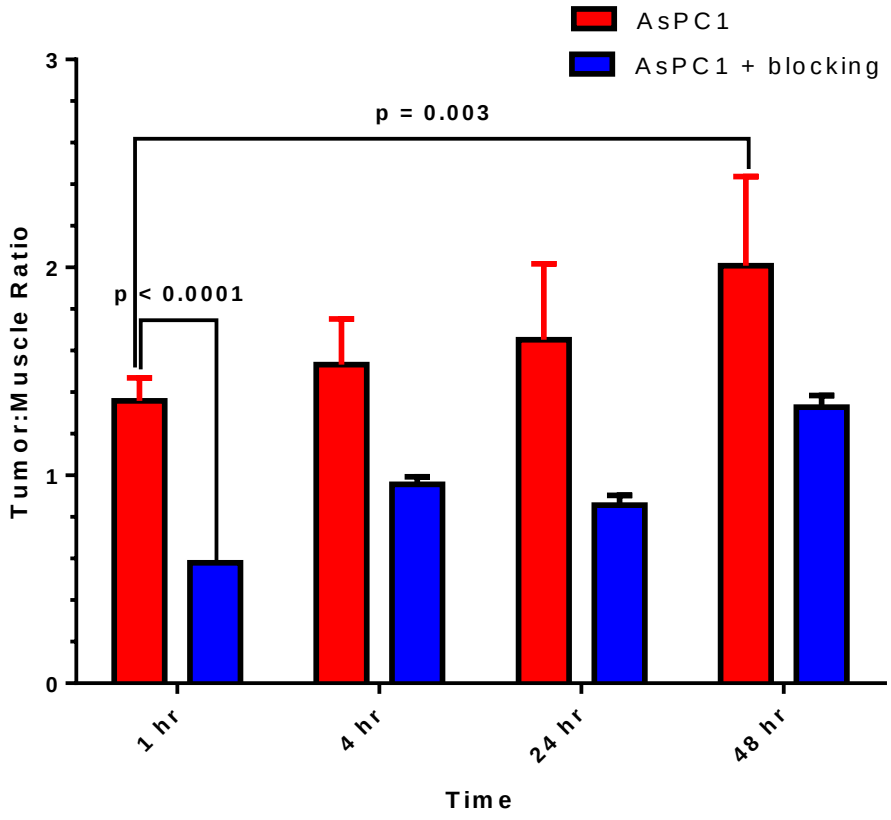

Figure 4.9 The change in tumor:muscle ratio after injection of SDA^{HER3}-D5A1-IRDye800 or SDA^{HER3}-D5A1-IRDye800 with x 20 fold excess of unlabeled SDA^{HER3}-D5A1 (as blocking agent) at 1 hours, 4 hours, 24 hours and 48 hours in PANC1 mouse xenograft model (Non-blocking: N = 3, Blocking: N = 2)

The tumor:muscle ratio from the PANC1 tumor increases over the time course. With blocking of unlabeled SDA^{HER3}-D5A1 proteins, the tumor:muscle ratio did not decrease, instead, all tumors with pre-blocking showed slightly increased in signals. No observation of increased tumor:muscle ratio during the experiment as observed in ASPC1 mouse xenograft model.

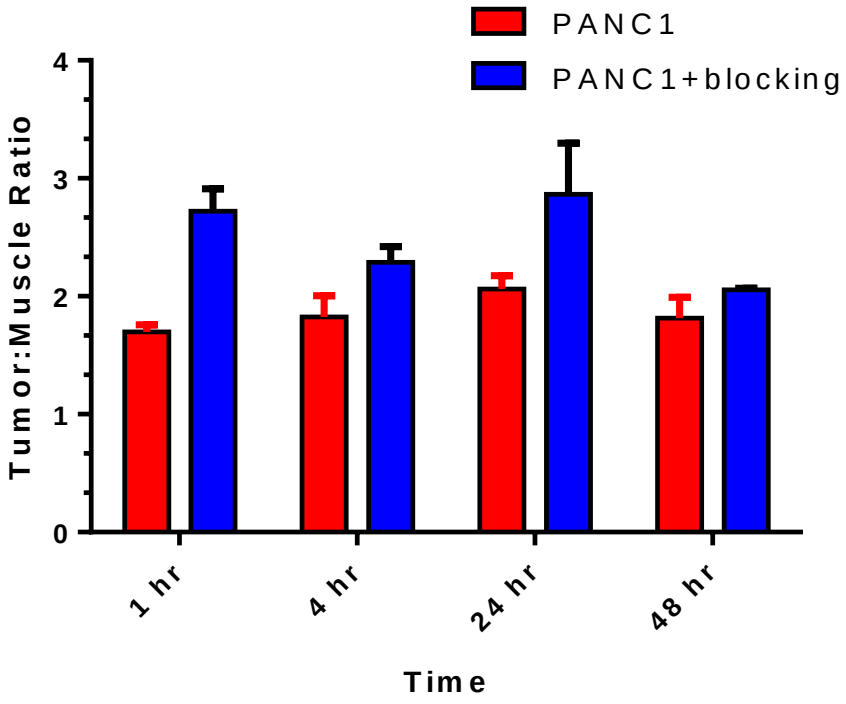

CHAPTER 5

General discussion

In the present study, novel FN3-based SDAs were selected through directed selection with mRNA display against ErbB3. In a similar study, Kronqvist and his colleagues identified several affibodies that bind to ErbB3 with nano and sub-nanomolar binding affinity through phage display[57]. In comparison of reported affibody and SDAs selected in our study, they all have similar binding affinity. Affibodies also have some cellular effects[56]. However, due to the limitation of phage display, the size of the affibody limited its application as therapeutic agents. So far, affibody has only been used as imaging agent for diagnosis in clinical trial[92]; while FN3-based protein Pegdinetanib has been in phase II clinical trials for treating glioblastoma, non-small cell lung cancer and colorectal cancer[93,94]. The major efforts for the ErbB3 targeting affibodies were contributed to the live animal imaging[81,91]. In contrast to the affibodies study, this study also focuses on the therapeutic effect of selected SDA^{HER3}s. To improve the biophysical property and affinity, the two selected SDA^{HER3}s (SDA^{HER3}-A1 and SDA^{HER3}-D5) were engineered into one biparatopic molecule (SDA^{HER3}-D5A1). The Cysteine residue at the C-terminus made the labeling and targeting easier by reaction and modification. The biparatopic molecule has picomolar affinity *in vitro* and selectively bind to the extracellular domain ErbB3 both *in vitro* and on cell surface. Therefore, the molecule is

promising for theranostic purpose. In the experiments, SDA^{HER3}-D5A1 demonstrated its capabilities in targeted delivery, addition effect with other drugs, as well as imaging for diagnosis. However, due to the limitations in experiments and time, this study did not explore the mechanism of the binding by crystal structures as Lee did for her study on an anti-ErbB3 antibody with the extracellular domain of ErbB3[95]. The proliferation assays and western blot analysis shed some lights on the mechanisms. It is hypothesized that the selected SDA^{HER3}s may be able to block the ligand binding of NRG1 and disrupt the dimerization of ErbB2 and ErbB3 (preliminary co-IP data was not shown here). It would be interesting to visualize how the selected SDA^{HER3}s interacts with the extracellular domain of ErbB3 and confirm the mechanisms of the molecule in disrupting the ligand-induced activation of downstream signaling pathways. For targeted delivery system, SDA^{HER3}-D5A1-Cys may be useful for targeted delivery of polymeric nanoparticles such as PLGA nanoparticles with toxins or small molecule drugs inside[96,97]. For therapeutic treatment, many of the anti-ErbB3 antibodies were used in combination with other antibodies/drugs in treating breast cancers or NSCLC. In clinical trials, MM-121 and trastuzumab were used together to treat trastuzumab-resistant patients[98]. MM-121 enhanced the effect of paclitaxel in ErbB2-overexpressing breast cancer[99]. MM-121 was combined with Cetuximab and inhibited tumor growth of head and neck cancers[100]. Thus, many other combinations of SDA^{HER3}-D5A1 and therapeutic agents can be tested with different types of ErbB3-overexpressing cancer cell lines. Meanwhile, mouse xenograft models are necessary to validate the cellular effect of SDA^{HER3}-D5A1 and the synergistic effect. For small animal imaging, the preliminary data showed some promising results. However, IRDye800 and current xenograft limited

the quality and reliability of the data. The PET imaging may be more helpful in quantify the efficiency and other mouse xenograft models should be tested to improve the results[101]. Besides biparatopic molecules, the future study may include the development of bispecific molecules. MEHD7945A is a bispecific antibody that targeting EGFR and ErbB3 with high affinity[102]. It showed anti-tumor effect with radiation and is currently in clinical trials[103]. Hackel and his colleagues identified an FN3-based protein that binds to EGFR through yeast display[104]. Therefore, it should be straightforward to combine the selected SDA^{HER3}s with this FN3-based EGFR binder through the similar approach for SDA^{HER3}-D5A1 construction. Other potential targets may be insulin growth factor (IGF1R)[105], VEGFR2[106], TNF-α[107] and Estrogen Receptor α[108], all of which have FN3-based protein binders. Overall, the flexibility of FN3 domain in protein engineering and high affinity to ErbB3 make SDA^{HER3}-D5A1 a good candidate for theranostic development.

REFERENCES

1. Loeb, K. R. & Loeb, L. a. Significance of multiple mutations in cancer. *Carcinogenesis* **21,** 379–385 (2000).

2. Hanahan, D. & Weinberg, R. A. Review Hallmarks of Cancer : The Next Generation. *Cell* **144,** 646–674 (2011).

3. Sawyers, C. Targeted cancer therapy. *Nature* **432,** 294–297 (2004).

4. Arora, a & Scholar, E. M. Role of tyrosine kinase inhibitors in cancer therapy. *J Pharmacol Exp Ther* **315,** 971–979 (2005).

5. Barouch-bentov, R. Mechanisms of Drug-Resistance in Kinases. *Expert Opin. Investig. Drugs* **20,** 153–208 (2012).

6. Zhang, J., Yang, P. L. & Gray, N. S. Targeting cancer with small molecule kinase inhibitors. *Nat Rev Cancer* **9,** 28–39 (2009).

7. Fedorov, O., Niesen, F. H. & Knapp, S. *Kinase Inhibitors*. *Kinase Inhibitors: Methods and Protocols, Method in Molecular Biology* **795,** (Humana Press, 2012).

8. Wu, P., Nielsen, T. E. & Clausen, M. H. FDA-approved small-molecule kinase inhibitors. *Trends Pharmacol. Sci.* **36,** 422–439 (2015).

9. Druker, B. J. *et al.* Efficacy and safety of a specific inhibitor of the BCR-ABL tyrosine kinase in chronic myeloid leukemia. *N. Engl. J. Med.* **344,** 1031–7 (2001).

10. Brief, N. I. N. FDA approves first PI3K inhibitor. *Nat. Rev. Drug Discov.* **13,** 644–645 (2014).

11. Wu, P., Nielsen, T. E. & Clausen, M. H. Small-molecule kinase inhibitors: an analysis of FDA-approved drugs. *Drug Discov. Today* **21,** 5–10 (2015).

12. Schlumberger, M. *et al.* Lenvatinib versus Placebo in Radioiodine-Refractory Thyroid Cancer. *N. Engl. J. Med.* **372,** 621–630 (2015).

13. Bixby, D. & Talpaz, M. Mechanisms of resistance to tyrosine kinase inhibitors in chronic myeloid leukemia and recent therapeutic strategies to overcome resistance. *Hematology Am. Soc. Hematol. Educ. Program* 461–76 (2009). doi:10.1182/asheducation-2009.1.461

14. Takeuchi, K. & Ito, F. Receptor Tyrosine Kinases and Targeted Cancer Therapeutics. *Biol. Pharm. Bull.* **34,** 1774–1780 (2011).

15. Gschwind, A., Fischer, O. M. & Ullrich, A. The discovery of receptor tyrosine kinases: targets for cancer therapy. *Nat. Rev. Cancer* **4,** 361–370 (2004).

16. Lemmon, M. A. & Schlessinger, J. Cell signaling by receptor tyrosine kinases. *Cell* **141,** 1117–1134 (2010).

17. Hynes, N. E. & Lane, H. A. ERBB receptors and cancer: the complexity of targeted inhibitors. *Nat. Rev. Cancer* **5,** 341–354 (2005).

18. Roskoski, R. The ErbB/HER family of protein-tyrosine kinases and cancer. *Pharmacol. Res.* **79,** 34–74 (2014).

19. Zhang, H. *et al.* ErbB receptors: from oncogenes to targeted cancer therapies. *J. Clin. Invest.* **117,** 2051–8 (2007).

20. Hynes, N. E. & MacDonald, G. ErbB receptors and signaling pathways in cancer. *Curr. Opin. Cell Biol.* **21,** 177–184 (2009).

21. Normanno, N. *et al.* Epidermal growth factor receptor (EGFR) signaling in cancer. *Gene* **366,** 2–16 (2006).

22. Bacus, S., Spector, N. & Yarden, Y. The era of ErbB-receptor-targeted therapies: advances toward personalized medicine. *Per. Med.* **2,** 301–315 (2005).

23. Ménard, S., Pupa, S. M., Campiglio, M. & Tagliabue, E. Biologic and therapeutic role of HER2 in cancer. *Oncogene* **22,** 6570–8 (2003).

24. Koutras, A. K. *et al.* The upgraded role of HER3 and HER4 receptors in breast cancer. *Crit. Rev. Oncol. Hematol.* **74,** 73–78 (2010).

25. Tovey, S. M., Dunne, B., Witton, C. J., Cooke, T. G. & Bartlett, J. M. S. HER4 in breast cancer: comparison of antibodies against intra- and extra-cellular domains of HER4. *Breast Cancer Res.* **8,** R19 (2006).

26. Sartor, C. I. *et al.* HER4 Mediates Ligand-Dependent Antiproliferative and Differentiation Responses in Human Breast Cancer Cells. *Mol. Cell. Biol.* **21,** 4265–4275 (2001).

27. Slamon, D. J. *et al.* Use of chemotherapy plus a monoclonal antibody against HER2 for metastatic breast cancer that overexpresses HER2. *N. Engl. J. Med.* **344,** 783–92 (2001).

28. Engelman, J. A. & Jänne, P. A. Mechanisms of acquired resistance to epidermal growth factor receptor tyrosine kinase inhibitors in non-small cell lung cancer. *Clin. Cancer Res.* **14,** 2895–2899 (2008).

29. Moasser, M. M. & Krop, I. E. The Evolving Landscape of HER2 Targeting in Breast Cancer. *JAMA Oncol.* **2,** (2015).

30. Sithanandam, G. & Anderson, L. M. The ERBB3 receptor in cancer and cancer gene therapy. *Cancer Gene Ther.* **15,** 413–448 (2008).

31. Campbell, M. R., Amin, D. & Moasser, M. M. HER3 Comes of Age: New Insights into Its Functions and Role in Signaling, Tumor Biology, and Cancer Therapy. *Clin. Cancer Res.* **16,** 1373–1383 (2010).

32. Gala, K. & Chandarlapaty, S. Molecular Pathways: HER3 Targeted Therapy. *Clin. Cancer Res.* **20,** 1410–1416 (2014).

33. Soltoff, S. P., Carraway, K. L., Prigent, S. A., Gullick, W. G. & Cantley, L. C. ErbB3 is involved in activation of phosphatidylinositol 3-kinase by epidermal growth factor. *Mol. Cell. Biol.* **14,** 3550–8 (1994).

34. Brown, K. K. & Toker, A. The phosphoinositide 3-kinase pathway and therapy resistance in cancer. *F1000Prime Rep.* **7,** 13 (2015).

35. Ma, J., Lyu, H., Huang, J. & Liu, B. Targeting of ErbB3 receptor to overcome resistance in cancer treatment. *Mol. Cancer* **13,** 105 (2014).

36. Engelman, J. A. *et al.* MET Amplification Leads to Gefitinib Resistance in Lung Cancer by Activating ERBB3 Signaling. *Science (80-.).* **316,** 1039–1043 (2007).

37. Gaborit, N., Lindzen, M. & Yarden, Y. Emerging anti-cancer antibodies and combination therapies targeting HER3/ERBB3. *Hum. Vaccin. Immunother.* **5515,** 1–17 (2015).

38. Xie, T. *et al.* Pharmacological targeting of the pseudokinase Her3. *Nat. Chem. Biol.* **10,** 1006–1012 (2014).

39. Littlefield, P., Moasser, M. M. & Jura, N. An ATP-competitive inhibitor modulates the allosteric function of the HER3 pseudokinase. *Chem. Biol.* **21,** 453–458 (2014).

40. Lim, S. M. *et al.* Development of small molecules targeting the pseudokinase Her3. *Bioorganic Med. Chem. Lett.* **25,** 3382–3389 (2015).

41. Treder, M. *et al.* 309 POSTER Fully human anti-HER3 mAb U3-1287 (AMG 888) demonstrates unique in vitro and in vivo activities versus other HER family inhibitors in NSCLC models. *Eur. J. Cancer Suppl.* **6,** 99 (2008).

42. Gala, K. & Chandarlapaty, S. Molecular pathways: HER3 Targeted therapy. *Clin. Cancer Res.* **20,** 1410–1416 (2014).

43. Garner, A. P. *et al.* An antibody that locks HER3 in the inactive conformation inhibits tumor growth driven by HER2 or neuregulin. *Cancer Res.* **73,** 6024–6035 (2013).

44. Higgins, M. J. & Baselga, J. Review series Targeted therapies for breast cancer. *J. Clin. Invest.* **121,** 3797–3803 (2011).

45. Fernandez-Cuesta, L. & Thomas, R. K. Molecular pathways: Targeting nrg1 fusions in lung cancer. *Clin. Cancer Res.* **21,** 1989–1994 (2015).

46. D'Souza, J. W. & Robinson, M. K. Oligoclonal antibodies to target the ErbB family. *Expert Opin. Biol. Ther.* **15,** 1015–1021 (2015).

47. Harris, R. C., Chung, E. & Coffey, R. J. in *The EGF Receptor Family* 3–14 (Elsevier, 2003). doi:10.1016/B978-012160281-9/50002-5

48. Packer, M. S. & Liu, D. R. Methods for the directed evolution of proteins. *Nat. Rev. Genet.* **16,** 379–394 (2015).

49. Cotten, S. W., Zou, J., Valencia, C. A. & Liu, R. Selection of proteins with desired properties from natural proteome libraries using mRNA display. *Nat. Protoc.* **6,** 1163–1182 (2011).

50. Wilson, D. S., Keefe, A. D. & Szostak, J. W. The use of mRNA display to select high-affinity protein-binding peptides. *Proc. Natl. Acad. Sci. U. S. A.* **98,** 3750–5 (2001).

51. Koide, A., Wojcik, J., Gilbreth, R. N., Hoey, R. J. & Koide, S. Teaching an old scaffold new tricks: monobodies constructed using alternative surfaces of the FN3 scaffold. *J. Mol. Biol.* **415,** 393–405 (2012).

52. Bloom, L. & Calabro, V. FN3: a new protein scaffold reaches the clinic. *Drug Discov. Today* **14,** 949–55 (2009).

53. Kim, D., Friedman, A. D. & Liu, R. Tetraspecific ligand for tumor-targeted delivery of nanomaterials. *Biomaterials* **35,** 6026–6036 (2014).

54. Kim, D., Yan, Y., Valencia, C. A. & Liu, R. Heptameric Targeting Ligands against EGFR and HER2 with High Stability and Avidity. *PLoS One* **7,** e43077 (2012).

55. Bravman, T., Bronner, V., Nahshol, O. & Schreiber, G. The ProteOn XPR36™ Array System—High Throughput Kinetic Binding Analysis of Biomolecular Interactions. *Cell. Mol. Bioeng.* **1,** 216–228 (2008).

56. Göstring, L. *et al.* Cellular effects of HER3-specific affibody molecules. *PLoS One* **7,** e40023 (2012).

57. Kronqvist, N. *et al.* Combining phage and staphylococcal surface display for generation of ErbB3-specific Affibody molecules. *Protein Eng. Des. Sel.* **24,** 385–396 (2011).

58. Ståhl, S. & Nygren, P. A. The use of gene fusions to protein A and protein G in immunology and biotechnology. *Pathol. Biol. (Paris).* **45,** 66–76 (1997).

59. Mamluk, R. *et al.* Anti-tumor effect of CT-322 as an adnectin inhibitor of vascular

endothelial growth factor receptor-2. *MAbs* **2,** 199–208

60. Jones, J. T., Akita, R. W. & Sliwkowski, M. X. Binding specificities and affinities of egf domains for ErbB receptors. *FEBS Lett.* **447,** 227–231 (1999).

61. Li, J. Y. *et al.* A Biparatopic HER2-Targeting Antibody-Drug Conjugate Induces Tumor Regression in Primary Models Refractory to or Ineligible for HER2-Targeted Therapy. *Cancer Cell* **29,** 117–129 (2016).

62. Fleetwood, F. *et al.* Simultaneous targeting of two ligand-binding sites on VEGFR2 using biparatopic Affibody molecules results in dramatically improved affinity. *Sci. Rep.* **4,** 7518 (2014).

63. Robert, B. *et al.* Tumor targeting with newly designed biparatopic antibodies directed against two different epitopes of the carcinoembryonic antigen (CEA). *Int. J. Cancer* **81,** 285–291 (1999).

64. Roovers, R. C. *et al.* A biparatopic anti-EGFR nanobody efficiently inhibits solid tumour growth. *Int. J. Cancer* **129,** 2013–2024 (2011).

65. Sheng, Q. *et al.* An Activated ErbB3/NRG1 Autocrine Loop Supports In Vivo Proliferation in Ovarian Cancer Cells. *Cancer Cell* **17,** 298–310 (2010).

66. Lee-Hoeflich, S. T. *et al.* A central role for HER3 in HER2-amplified breast cancer: Implications for targeted therapy. *Cancer Res.* **68,** 5878–5887 (2008).

67. Choi, B.-K., Fan, X., Deng, H., Zhang, N. & An, Z. ERBB3 (HER3) is a key sensor in the regulation of ERBB-mediated signaling in both low and high ERBB2 (HER2) expressing cancer cells. *Cancer Med.* **1,** 28–38 (2012).

68. Higgins, M. J. *et al.* A randomized, double-blind phase II trial of exemestane plus MM-121 (a monoclonal antibody targeting ErbB3) or placebo in postmenopausal women with locally advaned or metastatic ER+/PR+, HER2-negative breast cancer. *J. Clin. Oncol.* **32,** 587 (2014).

69. Lazrek, Y. *et al.* Anti-HER3 domain 1 and 3 antibodies reduce tumor growth by hindering HER2/HER3 dimerization and AKT-induced MDM2, XIAP, and FoxO1 phosphorylation. *Neoplasia* **15,** 335–47 (2013).

70. Grainger, D. W. Controlled-release and local delivery of therapeutic antibodies. *Expert Opin. Biol. Ther.* **4,** 1029–1044 (2004).

71. Diamant, E., Torgeman, A., Ozeri, E. & Zichel, R. Monoclonal Antibody Combinations that Present Synergistic Neutralizing Activity: A Platform for Next-Generation Anti-Toxin Drugs. *Toxins (Basel).* **7,** 1854–1881 (2015).

72. Brannon-Peppas, L. & Blanchette, J. O. Nanoparticle and targeted systems for cancer therapy. *Adv. Drug Deliv. Rev.* **64,** 206–212 (2012).

73. Wu, A. M. & Olafsen, T. Antibodies for molecular imaging of cancer. *Cancer J.* **14,** 191–7

74. Hudis, C. A. Trastuzumab — Mechanism of Action and Use in Clinical Practice. *N. Engl. J. Med.* **357,** 39–51 (2007).

75. Nahta, R. & Esteva, F. J. HER-2-targeted therapy: lessons learned and future directions. *Clin. Cancer Res.* **9,** 5078–84 (2003).

76. Verma, S. *et al.* Trastuzumab emtansine for HER2-positive advanced breast cancer. *N. Engl. J. Med.* **367,** 1783–91 (2012).

77. Swain, S. M. *et al.* Pertuzumab, Trastuzumab, and Docetaxel in HER2-Positive Metastatic Breast Cancer. *N. Engl. J. Med.* **372,** 724–734 (2015).

78. Sampath, L. *et al.* Dual-Labeled Trastuzumab-Based Imaging Agent for the Detection of Human Epidermal Growth Factor Receptor 2 Overexpression in Breast Cancer. *J. Nucl. Med.* **48,** 1501–1510 (2007).

79. Farokhzad, O. C., Karp, J. M. & Langer, R. Nanoparticle-aptamer bioconjugates for cancer targeting. *Expert Opin. Drug Deliv.* **3,** 311–24 (2006).

80. Terwisscha van Scheltinga, A. G. T. *et al.* ImmunoPET and biodistribution with human epidermal growth factor receptor 3 targeting antibody ^{89}Zr-RG7116. *MAbs* **6,** 1051–1058 (2014).

81. Rosestedt, M. *et al.* Affibody-mediated PET imaging of HER3 expression in malignant tumours. *Sci. Rep.* **5,** 15226 (2015).

82. Eichhorn, P. J. A. *et al.* Phosphatidylinositol 3-Kinase Hyperactivation Results in Lapatinib Resistance that Is Reversed by the mTOR/Phosphatidylinositol 3-Kinase Inhibitor NVP-BEZ235. *Cancer Res.* **68,** 9221–9230 (2008).

83. Wang, J. *et al.* [Effects of mammalian-target-of-rapamycin pathway on lapatinib resistance in breast cancer MDA-MB-231 cells]. *Zhonghua Yi Xue Za Zhi* **93,** 1915–7 (2013).

84. Konecny, G. E. *et al.* Activity of the dual kinase inhibitor lapatinib (GW572016) against HER-2-overexpressing and trastuzumab-treated breast cancer cells. *Cancer Res.* **66,** 1630–1639 (2006).

85. Xing, L., Hung, M., Bonfiglio, T., Hicks, D. G. & Tang, P. Breast Cancer : Basic and Clinical Research The Expression Patterns of ER , PR , HER2 , CK5 / 6 , EGFR , Ki-67 and AR by Immunohistochemical Analysis in Breast Cancer Cell Lines. *Breast Cancer Basic Clin. Res.* **4,** 35–41 (2010).

86. Shapira, A., Livney, Y. D., Broxterman, H. J. & Assaraf, Y. G. Nanomedicine for targeted cancer therapy: towards the overcoming of drug resistance. *Drug Resist.*

Updat. **14,** 150–63 (2011).

87. Chatterjee, D. K., Diagaradjane, P. & Krishnan, S. Nanoparticle-mediated hyperthermia in cancer therapy. *Ther. Deliv.* **2,** 1001–1014 (2011).

88. Xiao, Z. *et al.* A Potent HER3 Monoclonal Antibody That Blocks Both Ligand-Dependent and -Independent Activities: Differential Impacts of PTEN Status on Tumor Response. *Mol. Cancer Ther.* **15,** 689–701 (2016).

89. Maeda, H., Wu, J., Sawa, T., Matsumura, Y. & Hori, K. Tumor vascular permeability and the EPR effect in macromolecular therapeutics: A review. *J. Control. Release* **65,** 271–284 (2000).

90. Smith-Jones, P. M. *et al.* Imaging the pharmacodynamics of HER2 degradation in response to Hsp90 inhibitors. *Nat. Biotechnol.* **22,** 701–6 (2004).

91. Orlova, A. *et al.* Imaging of HER3-expressing xenografts in mice using a (99m)Tc(CO) 3-HEHEHE-Z HER3:08699 affibody molecule. *Eur. J. Nucl. Med. Mol. Imaging* **41,** 1450–9 (2014).

92. Gebauer, M. & Skerra, A. Engineered protein scaffolds as next-generation antibody therapeutics. *Curr. Opin. Chem. Biol.* **13,** 245–55 (2009).

93. Lipovsek, D. Adnectins: engineered target-binding protein therapeutics. *Protein Eng. Des. Sel.* **24,** 3–9 (2011).

94. Schiff, D. *et al.* Phase 2 study of CT-322, a targeted biologic inhibitor of VEGFR-2 based on a domain of human fibronectin, in recurrent glioblastoma. *Invest. New Drugs* **33,** 247–53 (2015).

95. Lee, S. *et al.* Inhibition of ErbB3 by a monoclonal antibody that locks the extracellular domain in an inactive configuration. *Proc. Natl. Acad. Sci.* **112,** 201518361 (2015).

96. Danhier, F. *et al.* PLGA-based nanoparticles: An overview of biomedical applications. *J. Control. Release* **161,** 505–522 (2012).

97. Kumari, A., Yadav, S. K. & Yadav, S. C. Biodegradable polymeric nanoparticles based drug delivery systems. *Colloids Surfaces B Biointerfaces* **75,** 1–18 (2010).

98. Huang, J. *et al.* The anti-ErbB3 antibody MM-121/SAR256212 in combination with trastuzumab exerts potent antitumor activity against trastuzumab-resistant breast cancer cells. *Mol. Cancer* **12,** 134 (2013).

99. Wang, S. *et al.* Therapeutic targeting of ErbB3 with MM-121/SAR256212 enhances antitumor activity of paclitaxel against ErbB2-overexpressing breast cancer. *Breast Cancer Res.* **15,** R101 (2013).

100. Jiang, N. *et al.* Combination of Anti-HER3 Antibody MM-121/SAR256212 and Cetuximab Inhibits Tumor Growth in Preclinical Models of Head and Neck Squamous Cell Carcinoma. *Mol. Cancer Ther.* **13,** 1826–1836 (2014).

101. ter Weele, E. J. *et al.* Imaging the distribution of an antibody-drug conjugate constituent targeting mesothelin with ^{89}Zr and IRDye 800CW in mice bearing human pancreatic tumor xenografts. *Oncotarget* **6,** 42081–90 (2015).

102. Kamath, A. V. *et al.* Preclinical pharmacokinetics of MEHD7945A, a novel EGFR/HER3 dual-action antibody, and prediction of its human pharmacokinetics and efficacious clinical dose. *Cancer Chemother. Pharmacol.* **69,** 1063–1069 (2012).

103. Li, C. *et al.* Antitumor Effects of MEHD7945A, a Dual-Specific Antibody against EGFR and HER3, in Combination with Radiation in Lung and Head and Neck Cancers. *Mol. Cancer Ther.* **14,** 2049–2059 (2015).

104. Hackel, B. J., Neil, J. R., White, F. M. & Wittrup, K. D. Epidermal growth factor receptor downregulation by small heterodimeric binding proteins. *Protein Eng. Des. Sel.* **25,** 47–57 (2012).

105. Chan, J. Y., Hackel, B. J. & Yee, D. Insulin receptor targeting in breast cancer through yeast surface display. *Cancer Res.* **75,** P4–06–02 (2015).

106. Getmanova, E. V *et al.* Antagonists to human and mouse vascular endothelial growth factor receptor 2 generated by directed protein evolution in vitro. *Chem. Biol.* **13,** 549–56 (2006).

107. Xu, L. *et al.* Directed evolution of high-affinity antibody mimics using mRNA display. *Chem. Biol.* **9,** 933–42 (2002).

108. Koide, A., Abbatiello, S., Rothgery, L. & Koide, S. Probing protein conformational changes in living cells by using designer binding proteins: Application to the estrogen receptor. *Proc. Natl. Acad. Sci.* **99,** 1253–1258 (2002).